THE JOURNAL OF BIOLOGICAL CHEMISTRY VOL. 289, NO. 26, pp. 18239–18257, June 27, 2014
© 2014 by The American Society for Biochemistry and Molecular Biology, Inc. Published in the U.S.A.

Transactivation of MicroRNA-320 by MicroRNA-383 Regulates Granulosa Cell Functions by Targeting E2F1 and SF-1 Proteins*

Received for publication, December 25, 2013, and in revised form, May 4, 2014 Published, JBC Papers in Press, May 14, 2014, DOI 10.1074/jbc.M113.546044

Mianmian Yin[‡§1], **Xiaorong Wang**[‡§1], **Guidong Yao**[¶], **Mingrong Lü**[‡§], **Meng Liang**[‡§], **Yingpu Sun**[¶2], **and Fei Sun**[‡§3]

From the [‡]*Institute of Immunology and Chinese Academy of Sciences Key Laboratory of Innate Immunity and Chronic Disease, Innovation Center for Cell Biology, School of Life Sciences and Medical Center, University of Science and Technology of China, Hefei, Anhui 230027, the* [§]*Hefei National Laboratory for Physical Sciences at Microscale, Hefei, Anhui 230027, and the* [¶]*Reproductive Medical Center, The First Affiliated Hospital of Zhengzhou University, Zhengzhou, Henan 450052, China*

Background: MicroRNAs are small noncoding RNAs associated with ovarian follicle development and female fertility.
Results: miR-320 inhibited estradiol synthesis and proliferation of granulosa cells (GCs) through targeting E2F1 and SF-1 *in vivo* and *in vitro*.
Conclusion: E2F1/SF-1 mediated miR-320-induced suppression of GC proliferation and of GC steroidogenesis.
Significance: These will potentiate the usefulness of miRNA in the treatment of some steroid-related disorders.

Our previous studies have shown that microRNA-320 (miR-320) is one of the most down-regulated microRNAs (miRNA) in mouse ovarian granulosa cells (GCs) after TGF-β1 treatment. However, the underlying mechanisms of miR-320 involved in GC function during follicular development remain unknown. In this study, we found that pregnant mare serum gonadotropin treatment resulted in the suppression of miR-320 expression in a time-dependent manner. miR-320 was mainly expressed in GCs and oocytes of mouse ovarian follicles in follicular development. Overexpression of miR-320 inhibited estradiol synthesis and proliferation of GCs through targeting E2F1 and SF-1. E2F1/SF-1 mediated miR-320-induced suppression of GC proliferation and of GC steroidogenesis. FSH down-regulated the expression of miR-320 and regulated the function of miR-320 in mouse GCs. miR-383 promoted the expression of miR-320 and enhanced miR-320-mediated suppression of GC proliferation. Injection of miR-320 into the ovaries of mice partially promoted the production of testosterone and progesterone but inhibited estradiol release *in vivo*. Moreover, the expression of miR-320 and miR-383 was up-regulated in the follicular fluid of polycystic ovarian syndrome patients, although the expression of E2F1 and SF-1 was down-regulated in GCs. These data demonstrated that miR-320 regulates the proliferation and steroid production by targeting E2F1 and SF-1 in the follicular development. Understanding the regulation of miRNA biogenesis and function in the follicular development will potentiate the usefulness of miRNA in the treatment of reproduction and some steroid-related disorders.

The ovary plays numerous roles that are critical for oocyte development and ovulation. The growing follicle is characterized by the increase in the oocyte size accompanied by the proliferation of surrounding GCs[4] (38). During ovarian folliculogenesis, the production of E_2 increases in quantity before ovulation and drops quickly immediately after ovulation (39). Within the ovary, GCs are the main sites for estrogen synthesis for local use as well as providing endocrine signaling to other tissues (1). The granulosa cells and theca cells of the ovary play central roles in regulating the growth and development of the oocyte to prepare for the surge of luteinizing hormone that promotes physiological responses leading to ovulation. These responses include promoting meiosis, follicular development, steroidogenesis, cumulus cell expansion, progesterone production and luteinization, ultimately promoting oocyte maturation and ovulation (2, 3).

Ovarian folliculogenesis is a complex and coordinated biological process that requires tightly regulated expression and the interaction of a multitude of genes. For example, SF-1 plays an important role in the development and function of the reproductive axis at multiple levels (4). SF-1 regulates cAMP-induced transcription from the proximal promoter (P II) of the *Cyp19a1* (the rate-limiting enzyme for estrogen synthesis) gene in the ovary (5). Adult knock-outs of SF-1 females were sterile, and their ovaries lacked corpora lutea (CL) and contained hemorrhagic cysts that resembled those in estrogen receptor α and aromatase KO mice (6). E2F1, an E2F family member, promotes the critical G_1-S phase transition stage and is involved in initiating the cell cycle (7–9). Besides the direct involvement of E2F1 in the cell cycle, the protein has been shown to stimulate apoptosis via p53-dependent (9) and -independent (10) mechanisms. In CHO cells, overexpression of E2F1 promotes growth

* This work was supported by National Natural Science Foundation of China Grants 31171379 and 81125005 (to F. S.), 31271605 (to Y. S.), and National Basic Research Program of China Grant 2014CB943100.
[1] Both authors contributed equally to this work.
[2] To whom correspondence may be addressed: School of Life Sciences, University of Science and Technology of China, Hefei, Anhui 230026, China. Tel.: 86-551-63600847; Cell phone: 13721100362; Fax: 86-551-63602703; E-mail: syp2008@vip.sina.com.
[3] To whom correspondence may be addressed: School of Life Sciences, University of Science and Technology of China, Hefei, Anhui 230026, China. Tel.: 86-551-63600847; Cell phone: 13721100362; Fax: 86-551-63602703. E-mail: feisun@ustc.edu.cn.

[4] The abbreviations used are: GC, granulosa cell; miR-320, microRNA-320; PND, postnatal day; E_2, estradiol; PCOS, polycystic ovarian syndrome; CL, corpora lutea; miRNA, microRNA; PMSG, pregnant mare serum gonadotropin; hCG, human chorionic gonadotropin; NC, negative control; LNA, locked nucleic acid; ISH, *in situ* hybridization; CCK-8, Cell Counting Kit-8; mGC, mouse GC; PARP, poly(ADP-ribose) polymerase; PCNA, proliferating cell nuclear antigen.

TABLE 1
PCR and RT-PCR primers used in this study

Gene	Forward primer sequence (5′ to 3′)	Reverse primer sequence (5′ to 3′)
Sf-1	GTATCCTCGAGCTATGGACTATTCGTACGACGAGG	GACATGAATTCTCAAGTCTGCTTGGCCTGCAGC
E2f1	GTATGAATTCTATGGCCGTAGCCCCCGCGG	CTAGGTCGACTCAGAAATCCAGAGGGGTCAGG
Sf-1 3′UTR	GCTTACTCGAGTGCCTCCAAAAGACTCCTTG	GTATAGCGGCCGCTTATAAGGGCACTTCTTGTC
E2f1 3′UTR	CTACTCTCGAGCAGAAGCCTAGGGATTCAGGGTG	CGAGCGCGGCCGCCATCAAAACATTTATTAAAATCAAAG
MiR-320 promoter(−2941/−48)	GTATCGAGCTCTCCACCTCCATATCTTCTTCCT	GTATCCTCGAGACCGTCGGATAAATACTATGGTC
MiR-320 promoter(−2019/−48)	GTATCGAGCTCTGTGAGCCAGTAAGTACACTAC	GTATCCTCGAGACCGTCGGATAAATACTATGGTC
miR-320 promoter(−1282/−48)	GTATCGAGCTCATCTCTAGGCCACACAACCTAA	GTATCCTCGAGACCGTCGGATAAATACTATGGTC
MiR-320 promoter(−998/−48)	GTATCGAGCTCACATCTACTGTTACACACATAAC	GTATCCTCGAGACCGTCGGATAAATACTATGGTC
MiR-320 promoter(−2019/−48) mutant form	GTGCTCATGACTGCAACAGTCCTGGGA	ACTGTTGCAGTCATGAGCACATCGAAA

during transition from serum-containing protein-free culture media and increases the density of viable cells (11, 12). Recently, microRNA (miRNA) has also indicated a critical role in the development of ovarian follicles by regulating genes involved in folliculogenesis (13–15).

miRNAs are small (19–25 bp) noncoding RNAs that post-transcriptionally control gene expression through their regulation of mRNA stability or translation (16). In the nucleus, miRNA precursors (pre-miRNA) are generated and exported to the cytoplasm where they are converted to mature miRNA. Mature miRNA, as part of an RNA-induced silencing complex, can pair with 3′UTRs of target mRNA and cause either mRNA degradation or translational repression (17, 18). The functions of miRNA have remained relatively unknown, and they are indicated as important cellular regulators that control development, growth, apoptosis, and differentiation (19). The roles of miRNAs in the ovary are shown by the fact that KO of Dicer, the ribonuclease III that plays critical roles in the synthesis of mature functional miRNA in the ovary, caused the dysfunction of folliculogenesis, oocyte maturation, ovulation, and infertility (20–24). miRNA populations have been investigated by cloning or next-generation sequencing of normal ovarian tissues from human (25), mice (26), and pigs (27) or ovarian carcinoma cells (28). Ro *et al.* (26) identified miRNA expression profiling in mouse ovaries and found that some miRNAs regulate the expression of genes that are critical for ovarian folliculogenesis and female fertility. TGF-β superfamily members have been shown to be involved in early follicle development (29) and GC proliferation or differentiation (30). We identified the miRNA signature of mouse pre-antral GCs after TGF-β1 treatment (14). The miRNA profiles in GCs indicated that three miRNAs were up-regulated and 13 miRNAs were down-regulated during TGF-β1 treatment. miR-224 is shown to promote GC proliferation and function through binding to the 3′UTR of Smad4. miRNA-383, one of the most significantly down-regulated miRNAs, is indicated to promote E_2 production in GCs (15). These studies suggest that miRNAs play an important role in the control of ovarian follicle development and female fertility. However, the precise mechanisms by which miRNAs or miRNA processing itself affect ovarian function and female fertility have not been well documented.

miR-320 is the second most significantly down-regulated miRNA. miR-320 has been shown to be involved in growth, proliferation, and the cell cycle by targeting different genes in different cell lines (31, 32). However, the functions and mechanisms of miR-320 in GC function during follicular development remain unclear. PCOS is the most common endocrinopathic disease in women of reproductive age and is the main cause of anovulatory infertility. In polycystic ovaries of anovulatory women, antral follicular development is obviously abnormal, and growth of these follicles is typically arrested before a mature follicle would be expected to ovulate (33). This aberration of follicular development seems to indicate an abnormal steroid environment. In ovulatory women, only a few oocytes will reach the preovulatory stage. The main feature of PCOS is hyperandrogenemia (34), and theca cells of polycystic ovaries have been shown to be the major source of excess androgens (35, 36). However, little is known about the reason for hyperandrogenemia in PCOS. In this study, miR-320 was functionally characterized in primary GCs and PCOS by identifying its target genes.

EXPERIMENTAL PROCEDURES

Experimental Animals and Follicular Fluid of Patients—ICR female mice were housed in the Animal Center, University of Science and Technology of China, and maintained under a light cycle (14 h light, 10 h dark) at room temperature (23 ± 2 °C). Mice were provided food and water *ad libitum*. All animal experiments were carried out in compliance with the rules of and approved by the institutional review boards of the University of Science and Technology of China.

Follicular fluid of patients (aged 20–40 years) with adenomyosis, endometriosis, endometrial polyps, PCOS ($n = 19$), and blocked fallopian tubes (normal controls, $n = 15$) were obtained from the First Affiliated Hospital of Zhengzhou University (Zhengzhou, China). All patients gave informed consent, and this study received ethical approval from the Institutional Review Boards of the University of Science and Technology of China and the Zhengzhou University.

Vectors—PEGFP-C1 vector was kindly donated by Mian Wu (University of Science and Technology of China), and the psi-CHECK-2 Dual-Luciferase reporter vector was kindly provided by Biliang Zhang (Guangzhou Institute of Biomedicine and Health, Chinese Academy of Sciences, Guangzhou, China). For the construction of expression plasmids, total RNA isolated from mouse liver and ovary tissue was reverse-transcribed to cDNA. The full-length cDNA was amplified by PCR applying RT-PCR primers indicated in Table 1.

The SF-1 expression constructs were generated by cloning the mouse cDNA into the pEGFP-C1 vector at the XhoI and EcoRI sites and pEGFP-E2F1 at the EcoRI and SalI sites. For construction of luciferase reporter plasmids, wild type *E2f1*

TABLE 2
Sequence of oligonucleotides

Oligonucleotides	Sequence (5′ to 3′)
Inhibitor NC	CAGUACUUUUGUGUAGUACAA
mmu-miR-320 inhibitors	UCGCCCUCUCAACCCAGCUUUU
mmu-miR-383 inhibitors	AGCCACAGUCACCUUCUGAUCU
Mimics NC	UUCUCCGAACGUGUCACGUTT ACGUGACACGUUCGGAGAATT
mmu-miR-320 mimics	AAAAGCUGGGUUGAGAGGGCGA GCCCUCUCAACCCAGCUUUUUU
mmu-miR-383 mimics	AGAUCAGAAGGUGACUGUGGCU CCACAGUCACCUUCUGAUCUUU
LNA scramble-miR	GTGTAACACGTCTATACGCCCA
LNA mmu-miR-320	TCGCCCTCTCAACCCAGCTTTT

3′UTR and wild type *Sf-1* 3′UTR were obtained by amplifying a 949-bp 3′UTR of the *E2f1* fragment and a 1250-bp 3′UTR of the *Sf-1* fragment harboring the miR-320-binding site predicted by the programs TargetScan, miRBase Targets, miRGen, and PicTar, respectively. Mutated *E2f1* 3′UTR and mutated *Sf-1* 3′UTR were generated by applying PCR-based site-directed mutagenesis. Wild type and mutated *E2f1* 3′UTR/*Sf-1* 3′UTR, were cloned into the XhoI and NotI sites of psiCHECK-2 reporter vector. The mouse miR-320 5′-flanking fragments of different lengths were amplified by PCR using mouse liver genomic DNA as a template, and oligonucleotide primers introduced a SacI and XhoI site at the 5′ and 3′end, respectively. The PCR products were digested with SacI and XhoI and then inserted into SacI and XhoI sites of the luciferase reporter plasmid pGL3-Basic (Promega, Madison, WI). Primer sequences are listed in Table 1. All constructs generated were verified by sequencing.

Reagents and Oligonucleotides—To prepare 1 mg/ml stock solutions, TGF-β1(R&D Systems, Minneapolis, MN) was reconstituted in acidified buffer containing 4 mM HCl (pH 5.7) and 1 mg/ml BSA (15). Purified human FSH (The National Hormone and Peptide Program, Torrance, CA) was reconstituted in PBS. Pregnant mare serum gonadotropin (PMSG) and human chorionic gonadotropin (hCG) were bought from Sigma. miR-320 mimics and inhibitors, miR-383 mimics and inhibitors, as well as scramble negative control (NC) were chemically synthesized and purified by Shanghai Gene-Pharma Co. (Shanghai, China). The miRNA mimics are double-stranded RNAs that mimic mature endogenous miRNA, and the miRNA inhibitors are single-stranded 2-*O*-methyl-modified oligoribonucleotide fragments that are exactly antisense to miRNA. Small interfering (si) RNAs (si-E2F1 and si-SF-1) were purchased from Santa Cruz Biotechnology, Inc. (Santa Cruz, CA). For the *in situ* hybridization (ISH) assay, the *Mus musculus* miR-320 locked nucleic acid (LNA) labeled with digoxigenin and scramble NC (LNA scrambled) were obtained from Exiqon A/S (Vedbaek, Denmark). LV3-pGLV-h1-GFP-puro-miR-320 mimics, LV3-pGLV-h1-GFP-puro-mimics NC, LV3-pGLV-h1-GFP-puro-miR-320 inhibitors sponge, and LV3-pGLV-h1-GFP-puro-inhibitors NC lentivirus were purchased from Shanghai Gene-Pharma Co. (Shanghai, China). Oligonucleotide sequences are listed in Table 2.

Follicle Isolation, Cell, Cell Culture, and Transfection—Preantral and antral follicles were isolated from postnatal day (PND) 10 and 25 mouse ovaries, respectively. Primary GCs were isolated and purified from pre-antral follicles of PND 10–12 mouse ovaries, as described by Yin *et al.* (15) and Yao *et al.* (14). Briefly, the ovaries were excised, and the follicles with a diameter of 90–110 μm were isolated using number 5 fine needles (Sigma). The isolated follicles were treated with type IV collagenase (Sigma) and TrypLE Express (Invitrogen), and the GCs were purified by washing and brief centrifugation. The isolated GCs were plated in DMEM/F-12 (1:1; Invitrogen) supplemented with 10% FBS (Invitrogen) and 1% antibiotics (100 units/ml penicillin and 100 μg/ml streptomycin; Invitrogen) at 37 °C with 5% CO_2. After 2 h of culture, nonadherent cells were removed by rinsing with culture medium. Culture media were replaced with fresh medium every 2 days thereafter, and the cells were used for experiments at two passages. To collect the CL, mice were first injected with PMSG (5 IU/mouse) for 48 h and then injected with hCG (5 IU/mouse). The CL were isolated from the ovaries with the aid of a dissecting microscope after the hCG injection for 24 h. HEK293T cells were cultured in DMEM supplemented with 10% FBS (Invitrogen) and 1% antibiotics (100 units/ml penicillin and 100 μg/ml streptomycin; Invitrogen) at 37 °C in a 5% CO_2 atmosphere. KGN (a human granulosa-like tumor cell line) was kindly donated by Dr. Yiming Mu (the General Hospital of the People's Liberation Army, Beijing, China). The KGN cell line was cultured under the same culture conditions as described in the primary GCs.

Primary GCs were transfected with either oligonucleotides or plasmids using HiPerFect transfection reagent (Qiagen GmbH, Hilden, Germany). Transfection was performed using Lipofectamine 2000 (Invitrogen) for HEK293T cells and Lipofectamine RNAiMAX (Invitrogen) for KGN cells. The transfection procedure was performed following the manufacturer's recommendations. Unless otherwise stated, cells were transfected with 50 nM indicated siRNA, 120 nM miR-320 mimics/miR-383 mimics, or 150 nM miR-320 inhibitors/miR-383 inhibitors.

Real Time PCR Analysis—Total RNA was isolated with TRIzol (Invitrogen) from ovaries, ovarian follicles, cultured cells, or follicular fluid (37) and then reverse-transcribed into cDNA using a PrimeScript RT reagent kit (TaKaRa Bio, Inc., Otsu, Japan) according to the manufacturer's instructions. Real time PCR was performed in ABI Step One System (Applied Biosystems, Foster City, CA) with the SYBR Premix Ex TaqII kit (TaKaRa Bio, Inc.), as described previously (14, 15). mRNA expression levels were normalized to *GAPDH* mRNA expression. Primer sequences are provided in Table 3. For mature mmu-miR-320, mmu-miR-383, and hsa-miR-383 detection, TaqMan microRNA assays (Applied Biosystems) were performed following the manufacturer's instructions. U6 snRNA (Applied Biosystems) was used for normalization.

Immunohistochemistry and ISH—The cellular localization of E2F1 and SF-1 proteins in the ovary was performed by immunohistochemical analysis, as described by Lian *et al.* (38). Briefly, mouse ovarian sections were incubated with the primary antibodies (anti-E2F1 (Santa Cruz Biotechnology) or anti-SF-1 (Millipore, Bedford, MA), both diluted at 1:200) overnight at 4 °C, followed by incubation with secondary antibody (Abcam, Cambridge, MA) for 2 h at room temperature. The immunosignals of E2F1 and SF-1 were visualized using streptavidin peroxidase with 3,3′-diaminobenzidine (Maixin Bio,

TABLE 3
Quantitative RT-PCR primers used in this study

Gene	Forward primer sequence (5′ to 3′)	Reverse primer sequence (5′ to 3′)
CYP19A1	TGTGTTGACCCTCATGAGACA	CTTGACGGATCGTTCATACTTTC
CYP11A1	TCCCTGTAAATGGGGCCATAC	AGGTCCTTCAATGAGATCCCTT
CYP17A1	GCCCAAGTCAAAGACACCTAAT	GTACCCAGGCGAAGAGAATAGA
GAPDH	TGTGTCCGTCGTGGATCTGA	TTGCTGTTGAAGTCGCAGGAG
Pri-miR-320	CTTCGTGACGCACCTGCGT	TTCGCCCTCTCAACCCAGCT
SF-1	ATGGCCGACCAGACCTTTATCTC	TGGTCCAACACCAGCAGCTC
E2F1	GGCTGGATCTGGAGACTGACC	CTGCACCTTCAGCACCTCAG

Fuzhou, China) as the chromogen. As a negative control, the primary antibody was omitted in parallel reactions.

Expression of miR-320 in the mouse ovary was performed by ISH using LNA-modified DNA probes on 8-μm frozen ovary sections, as described by Lian *et al.* (38). The probe sequences are provided in Table 2. In brief, ovarian cryosections from PND 1, 4, 10, 14, and 21, 1M and 2M mice and PND 21 mice after PMSG treatment were prehybridized for 4–6 h at 59 °C with 700 μl of prehybridization buffer (50% formamide, 5× saline sodium citrate, 5× Denhardt's, 200 μg/ml yeast RNA, 500 μg/ml salmon sperm DNA, 2% blocking reagents (Roche Applied Science), and diethyl pyrocarbonate-treated water). Sections were then covered with 150 μl of denatured hybridization buffer containing 1 pmol of LNA probes and incubated overnight at 52 °C in a humidified chamber. The hybridization signals were examined by utilizing anti-digoxigenin-alkaline phosphatase fragments of antigen-binding fragments (1:250; Roche Applied Science) and nitro blue tetrazolium/5-bromo-4-chloro-3-indolyl phosphate solution (Roche Applied Science).

Western Blotting—Cells and ovaries were lysed using radioimmunoprecipitation assay buffer (50 mM Tris-HCl (pH 7.4), 150 mM NaCl, 1% Triton X-100, 1% SDS, 1% sodium deoxycholate, and 1 mM EDTA) containing proteinase inhibitors (10 μg/ml each of aprotinin, pepstatin, and leupeptin) and 1 mM phenylmethylsulfonyl fluoride. The extraction of nuclear and cytoplasmic proteins in primary GCs were performed using NE-PER nuclear and cytoplasmic extraction reagents (Pierce) according to the manufacturer's specifications. Protein lysates were resolved by SDS-PAGE, electrically transferred to a Hybond ECL nitrocellulose membrane (Amersham Biosciences), immunoblotted with antibodies, and detected using enhanced chemiluminescence (Eastman Kodak). The primary antibodies used for immunoblotting were as follows: anti-E2F1 (Santa Cruz Biotechnology); anti-SF-1 (Millipore); anti-CYP19A1 (Abnova, Walnut, CA); anti-c-Myc (Cell Signaling Technology); anti-PARP (Cell Signaling Technology); anti-caspase-3 (Cell Signaling Technology); anti-Lamin A/C (Santa Cruz Biotechnology); anti-CDK4 (Abcam); anti-CDK2 (Abcam); and anti-cyclinD1 and anti-GAPDH (Santa Cruz Biotechnology).

Luciferase Reporter Assay—PsiCHECK2 and pGL3-Basic vectors were used in the luciferase reporter assays, as described by Yao *et al.* (14). HEK293T cells were transiently co-transfected with reporter constructs and the indicated plasmids, miR-320 mimics/inhibitors, or mmu-miR-383 mimics. Cells were harvested 30 h after transfection for reporter activity assay by using the Dual-Luciferase Reporter Assay System (Promega).

Cell Proliferation Assay and Hormone Analysis—Cell Counting Kit-8 (CCK-8) (Dojindo Laboratories, Kumamoto, Japan) was used to measure cell proliferation. Cells were plated in 96-well plates at 1–1.5 × 10^4 cells per well and cultured in the medium. At the indicated time points, the culture medium of each well was treated with 10 μl of the CCK-8 solution and then incubated for 2 h at 37 °C. The cell numbers were examined in triplicate by measuring the absorbance of each well at a wavelength of 450 nm (A_{450}) using a 96-well format plate reader (ELX 800 universal microplate Reader; BioTek, Inc., Highland Park, IL).

To determine the effects of miR-320 on GC steroidogenesis, GCs were transfected with oligonucleotides or plasmids. After 24 h, the medium was replaced with fresh DMEM/F-12 supplemented with 10% FBS and testosterone (Sigma) at 10^{-6} M, followed by continued culture for another 24 h. The serum samples were collected 3 days after lentivirus injection. E_2, progesterone, and testosterone concentrations in culture medium and serum were measured according to the manufacturer's instructions using the Access Immunoassay System (Beckman Coulter, Inc., Brea, CA), an automated random-access chemiluminescence-based assay. The intra- and interassay coefficients of variation were less than 10 and 15%, respectively.

Flow Cytometric Analysis—Apoptosis were detected using the FACSCalibur flow cytometer (BD Biosciences). Data analysis was performed using WinMDI 2.9 software (Scripps Research Institute, La Jolla, CA). Cells were seeded in 6-well plates at 30–50% confluency. Cells were harvested at 72 h after transfection with 120 nM miR-320 mimics/mimics NC or 150 nM miR-320 inhibitors/inhibitors NC, stained using the annexin V FITC Apoptosis detection kit (Beijing Biosea Biotechnology Co., Ltd., Beijing, China), and analyzed by flow cytometry.

miRNA Injection Technique—Mice were anesthetized using pentobarbital. A small dorsal abdominal incision was made in the lumbar region on each side of the midline (22). Through the incision in the dorsal abdominal wall, the ovaries and associated fat pad were gently pulled outside the body (22). The intrabursal injection was performed under microscopic magnification by inserting a 30-gauge needle with 2 × 10^7 transduction units of lentivirus through the ovarian fat pad into the ovarian bursa. The wound was sutured with silk when the ovaries were returned to the abdominal cavity. In each mouse, a 20-μl mixture of 1 × 10^7 transduction units of miR-320 mimics/mimics NC lentivirus and 5 × 10^7 transduction units of miR-320 inhibitors sponge/inhibitors NC lentivirus with normal saline and 5 μg/ml Polybrene was delivered into both ovaries. To determine the injection and infection efficiency, injection of mimics NC or

inhibitors NC lentivirus was used as a control. Animals were sacrificed 3 days after the injection, and the ovaries were sectioned, frozen, and examined under a fluorescent microscope with Hoechst staining. After lentivirus injection, the treated mice were housed separately and then were housed with a fertile male mouse for mating when they recovered normal behavioral activity.

Statistics—All experiments were repeated at least three times and performed in triplicate in this study. Data were presented as means ± S.E. Means of groups were compared with Student's *t* test and the one- or two-way analysis of variance test when appropriate. A p value <0.05 was considered statistically significant.

RESULTS

miR-320 Is Involved in the Follicular Development—In our previous studies on miRNA expression signature of mouse GCs (mGCs) treated with TGF-β1, miR-320 was the second most down-regulated miRNA (the other two are miR-500 and miR-383) (14). The real time PCR results showed that the expression of miR-320 was significantly suppressed in GCs stimulated by TGF-β1 (Fig. 1*A*), which validated the microarray data. Expression pattern of miR-320 in the mouse ovary was identified by real time PCR and ISH. PMSG treatment results in increased E_2 production and growth of the pre-ovulatory follicles of immature female mice. Furthermore, the administration of PMSG followed by hCG treatment mimics the enhancement of luteinizing hormone on progesterone production and inhibitory effect of luteinizing hormone on E_2 production (39, 40). In this study, the expression of miR-320 was significantly inhibited in the ovaries of immature female mice after 24, 48, and 72 h of PMSG treatment (Fig. 1*B*). In addition, hCG injection (24 h) after PMSG treatment (48 h) caused a rapid increase in miR-320 expression levels (Fig. 1*B*). The follicular diameter positively correlated with GC proliferation, E_2 secretion, and follicular growth (41); the real time PCR results revealed that the expression level of miR-320 in antral follicles was lower than that in pre-antral follicles but increased sharply after ovulation (Fig. 1*C*). The developmental changes of miR-320 expression in the mouse ovary were investigated by real time PCR and ISH using LNA-modified probes. miR-320 expression was mainly found in GCs and oocytes of follicles at various stages (Fig. 1*D*). The expression of miR-320 decreased in PMSG-treated immature mice (Fig. 1*D*), which was similar to the real time PCR results (Fig. 1*B*). miR-320 expression levels gradually declined with the development of ovaries (Fig. 1*E*). To exclude the possibility that down-regulation of miR-320 after PMSG treatment was directly inhibited by PMSG, the expression level of miR-320 was detected in GCs after PMSG treatment. No significant differences in the levels of miR-320 were observed between PMSG-treated and -untreated GCs (data not shown). Taken together, these results show that miR-320 may be involved in GC proliferation, GC function, oocyte development, and maturation during follicular development.

Steroidogenesis and proliferation are major functions of GCs in the developing follicles. We next examined the effect of miR-320 on GCs and KGN (human ovarian cancer cell line) cells by transfection of either miR-320 mimics or inhibitors into the mGCs and KGN cells for 48 h. Transfection with miR-320 mimics enhanced endogenous miR-320 levels by ~100-fold, whereas miR-320 inhibitors caused more than 50% decrease in mature miR-320 levels in GCs (data not shown). CCK-8 assay results demonstrated that miR-320 mimics significantly decelerated the proliferation of GCs (Fig. 1*F*) and KGN (data not shown) in a dose-dependent manner, whereas the miR-320 inhibitors increased cell proliferation (Fig. 1*G*). Hormone analysis results revealed that miR-320 mimics not only significantly suppressed E_2 synthesis (Fig. 1*H*) but also promoted progesterone production (Fig. 1*I*) in GCs. In contrast, silencing of miR-320 resulted in increased E_2 biosynthesis and decreased progesterone production. To exclude the possibility that the change in E_2 and progesterone levels was due to the cell proliferation stimulated by miR-320, variation in the expression levels of GAPDH in each group was examined. Cell extracts were immunoblotted for GAPDH protein levels. No significant differences in the levels of GAPDH were observed between treated and untreated cells (Fig. 1*H*). FACS results showed that overexpression of miR-320 significantly induced apoptosis of KGN (Fig. 1*J*). Conversely, inhibition of endogenous miR-320 with miR-320 inhibitors resulted in a significant suppression of basal apoptosis (Fig. 1*J*). Caspase-3 (a member of the caspase family of 13 aspartate-specific cysteine proteases) and PARP are shown to play important roles in the execution of the apoptotic program (42). In this study, endogenous PARP and caspase-3 were apparently cleaved in the KGN (Fig. 1*K*) and GCs (data not shown) transfected with miR-320 mimics, whereas the cleavage of PARP and caspase-3 was inhibited by miR-320 inhibitors (Fig. 1*K*). To address the mechanisms of the effects of miR-320 on the steroidogenesis in GCs, we detected *Cyp19a1*, *Cyp11a1*, and *Cyp17a1* (key enzyme in E_2 and progesterone biosynthesis) mRNA expression levels in GCs transfected with miR-320 mimics or inhibitors. Real time PCR and immunoblotting analysis showed that *Cyp19a1* mRNA and protein expression was significantly decreased in miR-320-transfected GCs, whereas inhibition of endogenous miR-320 enhanced Cyp19a1 mRNA and protein expression in GCs (Fig. 1, *L–N*). However, *Cyp11a1* and *Cyp17a1* mRNA levels were not affected in GCs after miR-320 treatment (Fig. 1*L*).

E2F1 and SF-1 Are Direct Targets of miR-320—Because miR-320 is mainly expressed in GCs and oocytes of different stage follicles, and significantly regulated steroid release and the proliferation of GCs, potential targets that modulate hormone synthesis and cell proliferation were predicted by the mi-Randa, PicTar, and TargetScan databases. Among the candidate miR-320 targets, we found that *E2f1* and *Sf-1* genes seem to be the most appropriate candidates, because E2F1 and SF-1 are indicated to promote proliferation in some types of cancer cells and regulate steroid synthesis in female mice (5, 11). The 3′UTR of *E2f1* mRNA contains an evolutionarily conserved miR-320 putative binding site in *M. musculus*, whereas the 3′UTR of *Sf-1* mRNA contains a poorly conserved miR-320 putative binding site in *M. musculus* (Fig. 2*A*). Immunoblotting and real time PCR analysis showed that both protein (Fig. 2, *B* and *C*) and mRNA (Fig. 2*D*) expressions of E2F1 and SF-1 were significantly suppressed in miR-320-transfected cells compared with the control cells, whereas the inhibition of miR-320 expression

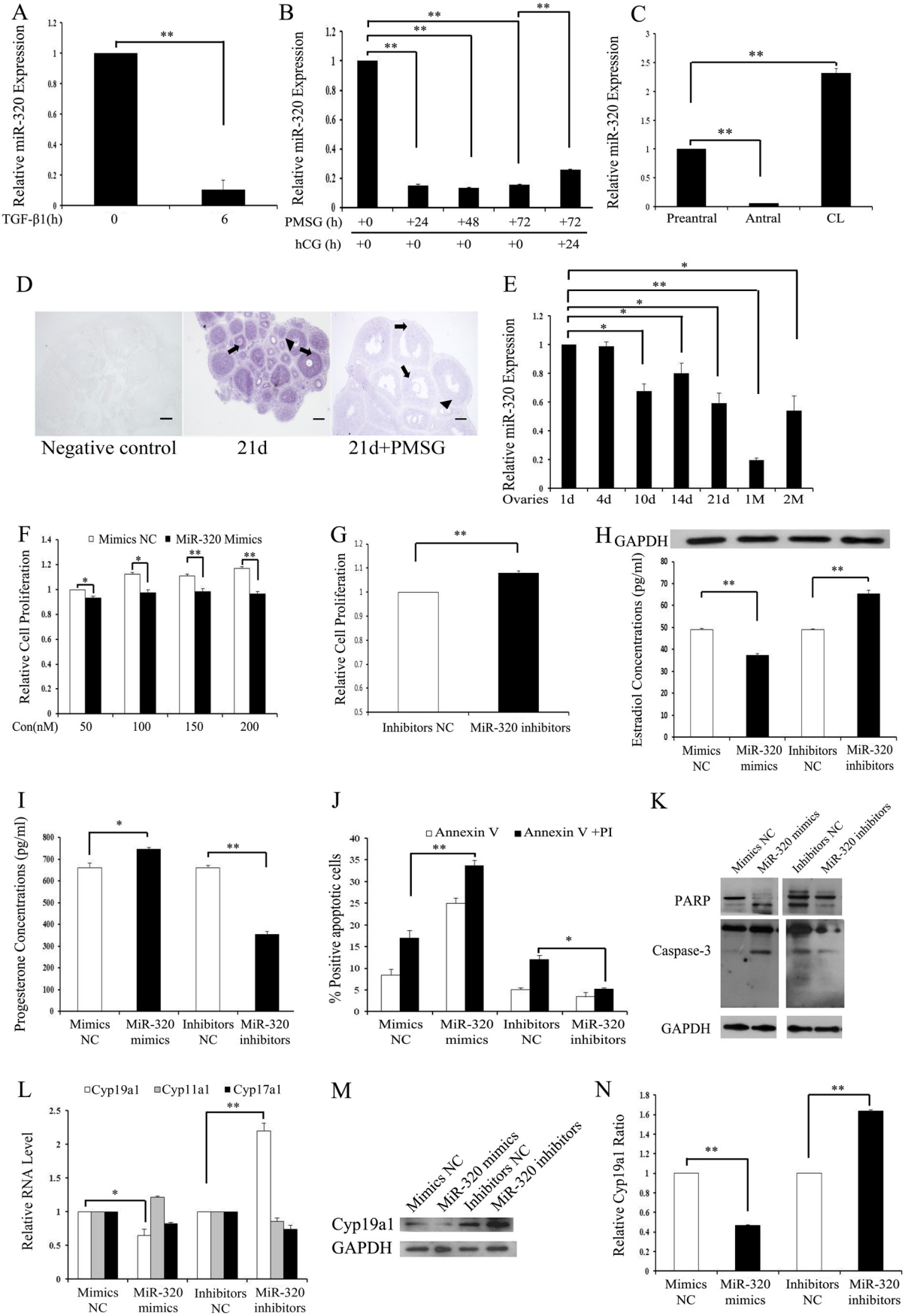
A
Relative miR-320 Expression
TGF-β1(h)
0
6
B
Relative miR-320 Expression
PMSG (h)
+0
+24
+48
+72
+72
hCG (h)
+0
+0
+0
+0
+24
C
Relative miR-320 Expression
Preantral
Antral
CL
D
Negative control
21d
21d+PMSG
E
Relative miR-320 Expression
Ovaries
1d
4d
10d
14d
21d
1M
2M
F
Mimics NC
MiR-320 Mimics
Relative Cell Proliferation
Con(nM)
50
100
150
200
G
Relative Cell Proliferation
Inhibitors NC
MiR-320 inhibitors
H
GAPDH
Estradiol Concentrations (pg/ml)
Mimics NC
MiR-320 mimics
Inhibitors NC
MiR-320 inhibitors
I
Progesterone Concentrations (pg/ml)
Mimics NC
MiR-320 mimics
Inhibitors NC
MiR-320 inhibitors
J
Annexin V
Annexin V +PI
% Positive apoptotic cells
Mimics NC
MiR-320 mimics
Inhibitors NC
MiR-320 inhibitors
K
Mimics NC
MiR-320 mimics
Inhibitors NC
MiR-320 inhibitors
PARP
Caspase-3
GAPDH
L
Cyp19a1
Cyp11a1
Cyp17a1
Relative RNA Level
Mimics NC
MiR-320 mimics
Inhibitors NC
MiR-320 inhibitors
M
Mimics NC
MiR-320 mimics
Inhibitors NC
MiR-320 inhibitors
Cyp19a1
GAPDH
N
Relative Cyp19a1 Ratio
Mimics NC
MiR-320 mimics
Inhibitors NC
MiR-320 inhibitors

was able to increase E2F1 and SF-1 expression in GCs (Fig. 2, *B–D*) and KGN (data not shown). These results show that miR-320 down-regulates E2F1 and SF-1 expression through decreasing their mRNA stability.

To further validate whether the *E2f1* and *Sf-1* genes are direct targets of miR-320, we constructed *Renilla* luciferase reporter vectors containing the wild type full-length of *E2f1* and *Sf-1* 3′UTR as well as mutant forms of the miR-320 seed sites. As shown in Fig. 2*E*, the luciferase activities of the wild type *E2f1* and **Sf-1** 3′UTR were significantly reduced with miR-320 mimics, whereas miR-320 inhibitors were able to significantly promote luciferase activities. However, the luciferase reporter activities of mutant forms of seeding sites were not inhibited by miR-320 (Fig. 2*F*). These results indicate that miR-320 down-regulates E2F1 and SF-1 expression through directly binding to their 3′UTRs.

Because there was a stronger signal in the nucleus than in the cytoplasm of the oocyte and GCs (Fig. 2*G*), we identified whether miR-320 regulates E2F1 and SF-1 in the nucleus or in the cytoplasm of GCs. Immunoblotting results show that miR-320 inhibited E2F1 and SF-1 expression in the nucleus, whereas the protein expression levels of E2F1 and SF-1 were not altered in the cytoplasm of GCs treated with miR-320 mimics/mimics NC (Fig. 2*H*). These results demonstrated that miR-320 mainly regulated the target gene expression in the nucleus.

We next studied the functional relevance of E2F1 and SF-1 in miR-320-mediated effects in GCs. The immunohistochemistry results demonstrated that E2F1 and SF-1 were mainly expressed in GCs and oocytes at various stages of follicular development (Fig. 2*I*), which was very similar to the expression pattern of miR-320 in the ovary. The co-localization of miR-320 with E2F1 and SF-1 protein indicates that they may interact with each other in mGCs. Knockdown of E2F1/SF-1 (si-E2F1/SF-1) (data not shown) and enforced E2F1/SF-1 expression significantly suppressed and increased GC proliferation (data not shown). Furthermore, overexpression of E2F1/SF-1 partially rescued miR-320-mediated inhibition of GC proliferation (Fig. 2*J*), although knockdown of E2F1/SF-1 (Fig. 2*K*) enhanced effects of miR-320 on GC proliferation. Hormone analysis results revealed that miR-320 mimics not only significantly attenuated SF-1-induced E_2 synthesis (Fig. 2*L*) but also rescued SF-1-mediated progesterone suppression (Fig. 2*M*) in GCs. The expression of E2F1/SF-1/CYP19a1 was significantly increased in the ovaries of immature female mice after 24, 48, and 72 h of PMSG treatment (Fig. 2, *N* and *O*). In addition, hCG injection (24 h) after PMSG treatment (48 h) resulted in the inhibition of E2F1/SF-1/CYP19a1 expression. The patterns of E2F1/SF-1/CYP19A1 protein expression levels in the ovaries were negatively correlated with the changes of miR-320 in PMSG/hCG-treated immature mice. The immunoblotting results showed that the expression of E2F1 and SF-1 increased accompanied by the ovarian development stage (Fig. 2, *P* and *Q*), which was negatively correlated with the expression of miR-320. Taken together, these results further suggest that E2F1 and SF-1 are real targets of miR-320 and mediate, at least in part, the functions of miR-320 in ovarian development.

FSH Regulates the Expression of miR-320, E2F1, and SF-1—FSH is the major regulator of folliculogenesis, particularly in driving proliferation and steroidogenesis of GCs (44). These physiological functions of FSH are achieved by the activation of different target genes in GCs (45). Because miR-320 regulates proliferation and steroidogenesis of GCs, we first examined whether miR-320 was involved in FSH-induced GC proliferation and steroidogenesis. The real time PCR results revealed that FSH treatment resulted in the inhibition of miR-320 expression (Fig. 3, *A* and *B*). Furthermore, overexpression of miR-320 partially attenuated FSH/serum-induced cell proliferation in GCs (Fig. 3, *C* and *D*). These results show that miR-320 might be involved in FSH/serum-induced cell proliferation. Second, the immunoblotting results show that FSH promoted the expression of E2F1 and SF-1 in a time-dependent manner (Fig. 3, *E* and *F*). Meanwhile, miR-320 mimics inhibited serum/FSH-inducible E2F1 and SF-1 protein expression (Fig. 3, *G–J*). The expression patterns for miR-320 and E2F1/SF-1 indicate that miR-320 might be involved in the regulation of E2F1 and SF-1 in FSH/serum-treated GCs.

miR-320 Regulates the Expression of E2F1 and SF-1 in Vivo—To evaluate the role of miR-320 on proliferation and steroidogenesis of GCs *in vivo*, the miRNAs were injected into female mouse ovaries. miR-320 mimics and miR-320 inhibitor sponges were constructed into the LV3-pGLV-h1-GFP-puro vectors. Green fluorescence of LV3-pGLV-h1-GFP-puro vectors were

FIGURE 1. **miR-320 regulates cell proliferation and steroidogenesis in mouse ovarian GCs.** *A,* TGF-β1 inhibited miR-320 expression in GCs. mGCs were treated with TGF-β1 (5 ng/ml) for 0 and 6 h and then subjected to real time PCR analysis. *B,* changes of miR-320 expression in ovaries of PMSG/hCG-treated immature mice. Total RNA was extracted from the ovaries of PMSG (20 IU)-treated mice at 0, 24, 48, or 72 h and PMSG/hCG-treated mice at the indicated post-hCG time points and then subjected to real time PCR analysis. *C,* miR-320 expression levels in pre-antral, antral, and CL. Total RNA was extracted from pre-antral, antral, and CL and then subjected to real time PCR. The expression of miR-320 in the pre-antral follicles was arbitrarily set at 1.0. *D,* miR-320 is mainly expressed in GCs (*arrow*) and oocytes (*arrowhead*) of ovarian follicles at various developmental stages. The localization of miR-320 was performed on 8-μm frozen ovarian sections of PND 21 and PMSG-treated mice by ISH using LNA-modified DNA probe complementary to miR-320. *Purple* denotes hybridization signals for miR-320. *Scale bar,* 100 μm. *d*, day. *E,* miR-320 expression in ovaries of PND 1, 4, 10, 14, 21, 1M, and 2M mice. Total RNA was extracted from the ovaries of PND 1, 4, 10, 14, 21, 1M, and 2M mice and then subjected to real time PCR analysis. The expression of miR-320 in the ovary of PND 1 mice was arbitrarily set at 1.0. *F* and *G,* overexpression and knockdown of miR-320 significantly inhibited and stimulated GC proliferation, respectively. Cell viability was measured by the CCK-8 assay after transfection with 50, 100, 150, or 200 nM miR-320 mimics and mimics NC or with 150 nM miR-320 inhibitors and inhibitors NC. *H* and *I,* miR-320 significantly repressed E_2 secretion and promoted progesterone release from GCs. GCs were transfected with 120 nM miR-320 mimics and mimics NC or 150 nM miR-320 inhibitors and inhibitors NC. After 48 h of culture, media were collected for the measurement of E_2 and progesterone levels, and cell lysate was used for the detection of GAPDH expression by Western blotting. *J,* miR-320 increased cell apoptosis. The apoptosis rate was analyzed using flow cytometry with annexin V and propidium iodide staining after transfection either with 100 nM miR-320 mimics/mimics NC or with 150 nM miR-320 inhibitors/inhibitors NC for 48 h. *K,* miR-320 regulated the expression of caspase-3 and PARP. Cells were transfected with oligonucleotides as described in *J*. The protein expressions of caspase-3 and PARP were determined by Western blotting. *L–N*, miR-320 reduces *Cyp19a1* mRNA (*L*) and protein (*M* and *N*) expression levels in mGCs. GCs were transfected with oligonucleotides as described in *H*. The mRNA expression of *Cyp19a1*, *Cyp17a1*, and *Cyp11a* and protein expression of CYP19A1 were determined by real time PCR and Western blotting, respectively. Representative Western blotting for CYP19A1 (*upper bands*) and GAPDH (*lower bands*) (*M*) and the corresponding densitometric analysis (*N*) are shown. *A–C, E–J, L*, and *N*, data represent the mean ± S.E. of three independent experiments performed in triplicate. *, $p < 0.05$; **, $p < 0.01$. *Con,* concentration.

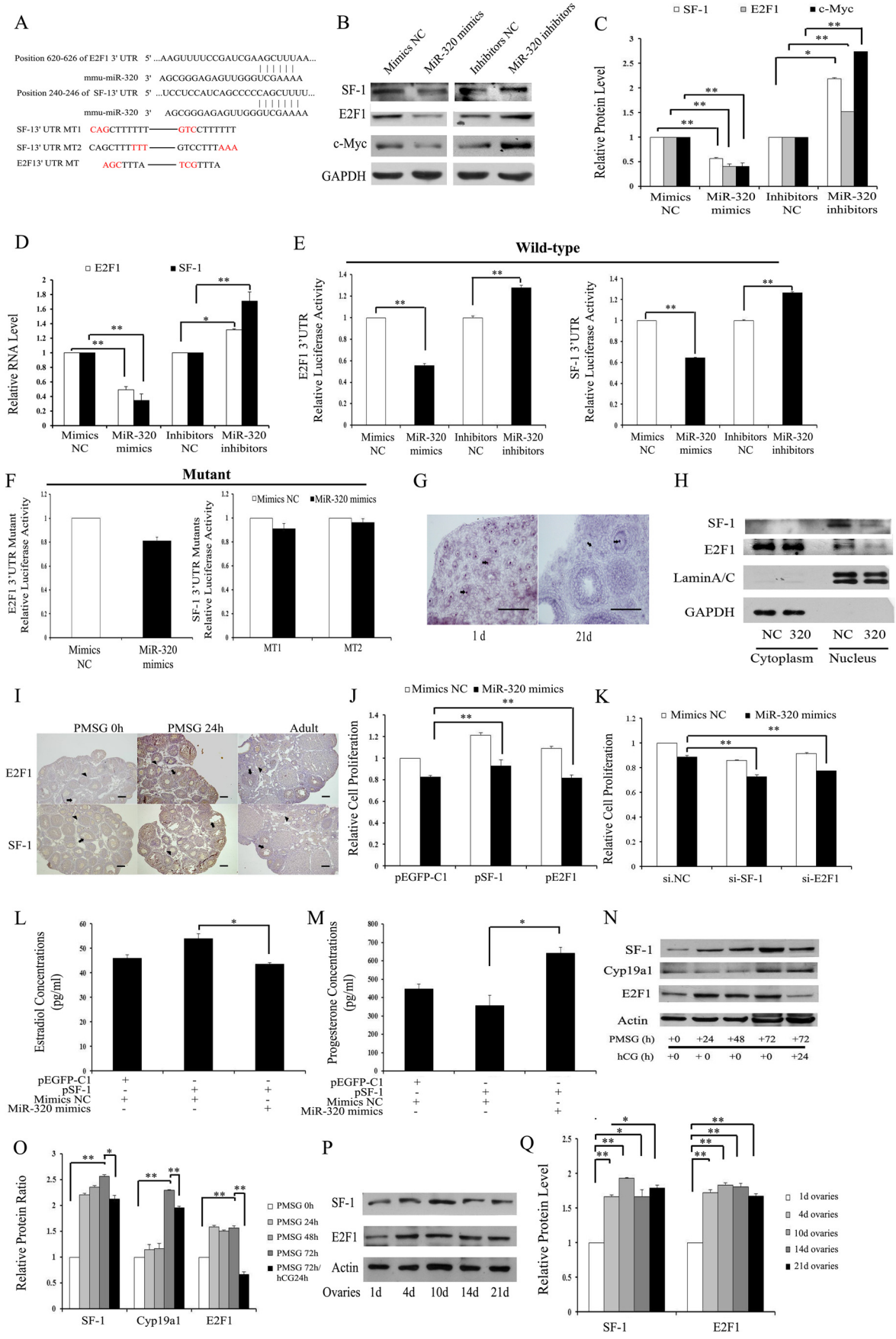
A
Position 620-626 of E2F1 3' UTR 5' ...AAGUUUUCCGAUCGAAGCUUUAA...
mmu-miR-320 3' AGCGGGAGAGUUGGGUCGAAAA
Position 240-246 of SF-13' UTR 5' ...UCCUCCAUCAGCCCCCAGCUUUU...
mmu-miR-320 3' AGCGGGAGAGUUGGGUCGAAAA
SF-13' UTR MT1 CAGCTTTTTT——GTCCTTTTTT
SF-13' UTR MT2 CAGCTTTTTT——GTCCTTTAAA
E2F13' UTR MT AGCTTTA——TCGTTTA
B
Mimics NC
MiR-320 mimics
Inhibitors NC
MiR-320 inhibitors
SF-1
E2F1
c-Myc
GAPDH
C
SF-1
E2F1
c-Myc
Relative Protein Level
Mimics NC
MiR-320 mimics
Inhibitors NC
MiR-320 inhibitors
D
E2F1
SF-1
Relative RNA Level
Mimics NC
MiR-320 mimics
Inhibitors NC
MiR-320 inhibitors
E
Wild-type
E2F1 3'UTR Relative Luciferase Activity
SF-1 3'UTR Relative Luciferase Activity
Mimics NC
MiR-320 mimics
Inhibitors NC
MiR-320 inhibitors
F
Mutant
E2F1 3'UTR Mutant Relative Luciferase Activity
SF-1 3'UTR Mutants Relative Luciferase Activity
Mimics NC
MiR-320 mimics
MT1
MT2
G
1 d
21d
H
SF-1
E2F1
LaminA/C
GAPDH
NC 320 NC 320
Cytoplasm
Nucleus
I
PMSG 0h
PMSG 24h
Adult
E2F1
SF-1
J
Mimics NC
MiR-320 mimics
Relative Cell Proliferation
pEGFP-C1
pSF-1
pE2F1
K
Mimics NC
MiR-320 mimics
Relative Cell Proliferation
si.NC
si-SF-1
si-E2F1
L
Estradiol Concentrations (pg/ml)
pEGFP-C1
pSF-1
Mimics NC
MiR-320 mimics
M
Progesterone Concentrations (pg/ml)
pEGFP-C1
pSF-1
Mimics NC
MiR-320 mimics
N
SF-1
Cyp19a1
E2F1
Actin
PMSG (h) +0 +24 +48 +72 +72
hCG (h) +0 +0 +0 +0 +24
O
Relative Protein Ratio
SF-1
Cyp19a1
E2F1
PMSG 0h
PMSG 24h
PMSG 48h
PMSG 72h
PMSG 72h/ hCG24h
P
SF-1
E2F1
Actin
Ovaries 1d 4d 10d 14d 21d
Q
Relative Protein Level
SF-1
E2F1
1d ovaries
4d ovaries
10d ovaries
14d ovaries
21d ovaries

used as a marker of infection efficiency. The labeled vectors were distributed in the whole ovaries, although the transduction efficiency of different cell type components was inconsistent in the treated ovaries (Fig. 4*A*). The real time PCR results showed that miR-320 levels were increased by ~3-fold in the ovaries injected with miR-320 mimics lentivirus, whereas miR-320 inhibitors sponge lentivirus caused a more than 50% decrease in the miR-320 levels of the treated GCs and ovaries (Fig. 4, *B* and *C*). Immunoblotting and real time PCR analysis showed that the mRNA (Fig. 4*C*) and protein (Fig. 4*D*) expression of E2F1 and SF-1 were significantly decreased in miR-320 mimics lentivirus-injected ovaries compared with the control ovaries, whereas the knockdown of miR-320 was able to induce E2F1 and SF-1 expression (Fig. 4, *C* and *D*). Because miR-320 regulates the proliferation and steroidogenesis *in vitro*, the genes involved in the proliferation, cell cycle, and apoptosis were determined by immunoblotting. The immunoblotting results showed that miR-320 inhibited the expression of PCNA and CDK4, which was involved in cell proliferation and the cell cycle (Fig. 4*D*), whereasthe miR-320 inhibitor sponge was able to promote PCNA and CDK4 expression (Fig. 4*D*). In this study, endogenous PARP and caspase-3 were apparently cleaved in the ovaries injected with miR-320 mimics lentivirus (Fig. 4*D*), whereas the cleavage of PARP and caspase-3 were inhibited by the miR-320 inhibitor sponge (Fig. 4*D*). These results indicated that miR-320 promotes the apoptosis of ovaries *in vivo*. Consistent with the results *in vitro*, E_2 levels were lower in miR-320 mimics lentivirus-treated mice than in mimics NC lentivirus-treated mice (Fig. 4*E*), although the levels of progesterone (Fig. 4*F*) and testosterone (Fig. 4*G*) were increased in miR-320 mimics lentivirus-treated mice. The inhibition of miR-320 by miR-320 inhibitor sponge lentivirus in mice significantly induced E_2 production (Fig. 4*E*) and impaired the secretion of progesterone (Fig. 4*F*) and testosterone (Fig. 4*G*). On the day following the lentivirus injection, the female mice were housed with fertile males, and they typically mated within 5 days of lentivirus treatment. miR-320 mimics lentivirus-injected mice were fertile and produced viable offspring (data not shown). Taken together, these results indicate that miR-320 inhibits the proliferation and production of E_2, while promoting the production of progesterone and testosterone, likely in part through the suppression of E2F1 and SF-1 expression *in vivo* and *in vitro*.

miR-383 Promotes the Expression of miR-320 and Enhances the Function of miR-320 on Cell Proliferation—The expression of miR-383 and miR-320 was suppressed in GCs treated with TGF-β1. Our previous studies have shown that miR-383 inhibits NTERA-2 (testicular embryonal carcinoma) cell proliferation by partially targeting *E2f1*, which is the direct target gene of miR-320. Similar to the expression pattern of miR-320, miR-383 expression was also mainly expressed in GCs and oocytes of follicles at various stages (15). The similar expression patterns and functions of miR-320 and miR-383 indicate that they might interact with each other in mGCs. As shown in Fig. 5, *A*, *C*, and *E*, miR-383 significantly promoted the expression of miR-320 and primary miR-320 *in vivo* and *in vitro*, while having no effect on the expression of miR-224. miR-383 inhibitors decreased miR-320 expression (Fig. 5*B*), whereas miR-320 had no effect on miR-383 expression (Fig. 5*D*). These results indicate that miR-383 regulates miR-320 expression at the transcriptional level. According to miRBase, the mouse miR-320 gene is an intergenic miRNA on chromosome 14. Intergenic miRNAs usually have their own transcription units and are transcribed with their own RNA polymerase II-like promoter (46). As shown in Fig. 5*F*, miR-383 overexpression increased the activity of the miR-320 promoter region by 1.5–2-fold, suggesting that miR-383 acts as a transcriptional activator of the miR-320 promoter. To further investigate the transcriptional regulation of

FIGURE 2. ***E2f1* and *Sf-1* are direct targets of miR-320.** *A,* putative binding sites for mmu-miR-320 are predicted in the 3′UTR of *E2f1* and *Sf-1* mRNA. The *underlined* nucleotides indicate the mutated bases of predicted miR-320-binding sites. *E2f1 3′UTR MT*, *E2f1* 3′UTR mutation type; *Sf-1 3′UTR MT*, *Sf-1* 3′UTR mutation type. *B–D,* miR-320 reduces E2F1, SF-1, and c-Myc protein (*B* and *C*) and mRNA (*D*) expression levels in mGCs. GCs were transfected with oligonucleotides as described in Fig. 1. The mRNA and protein expression of E2F1, SF-1, and c-Myc were determined by real time PCR and Western blotting, respectively. Representative Western blotting for SF-1 (*upper bands*), E2F1 (*upper middle bands*), c-Myc (*lower middle bands*), and GAPDH (*lower bands*) (*B*) and the corresponding densitometric analysis (*C*) are shown. The ratio of the SF-1/E2F1/c-Myc band intensity over the GAPDH band intensity in controls was arbitrarily set at 1.0. *E* and *F,* effect of miR-320 on E2F1 and SF-1 3′UTR luciferase activities. miR-320 mimics inhibit E2F1 and SF-1 (*E*) 3′UTR luciferase activities. In contrast, knockdown of miR-320 (*E*) or seed mutant (*F*) forms of miR-320 could no longer inhibit reporter luciferase activities. Cells were co-transfected with wild type (*WT*) E2F1 and SF-1 (*E*) 3′UTR or mutant E2F1 and SF-1 (*F*) 3′UTR reporter constructs and miR-320 mimics/mimics NC, or miR-320 inhibitors/inhibitors NC. After 30 h of transfection, Firefly luciferase activity and *Renilla* luciferase activity were measured. The value from cells co-transfected with mimics NC and plasmid expressing WT E2F1/SF-1 3′UTR was arbitrarily set at 1. *G,* miR-320 expression in the nucleus (*arrowhead*) of GCs and oocytes. The localization of miR-320 was performed as described in Fig. 1*D*. *Purple* denotes hybridization signals for miR-320. *Scale bar,* 100 μm. *H,* Western blotting analysis of SF-1 and E2F1 expression in the nucleus and cytoplasm. Lysates from mouse GCs transfected with miR-320 mimics/mimics NC were separated into cytosolic and nuclear fractions and then immunoblotted with antibodies against SF-1, E2F1, lamin A/C, and GAPDH. Lamin A/C and GAPDH were used as markers for nuclear and cytoplasmic fractions, respectively. *I,* immunohistochemical staining for E2F1 and SF-1 in the ovaries from immature mice that were either untreated (*PMSG 0 h*) or treated with PMSG for 24 h (*PMSG 24 h*), and from adult mice. E2F1 and SF-1 proteins (stained *brown*) are mainly located in GCs (*arrowhead*) and oocytes (*arrow*) at different stages of follicular development. *Scale bar,* 50 μm. *J,* overexpression of E2F-1 or SF-1 partially rescued miR-320-induced proliferation suppression. Cell viability was analyzed after co-transfection with miR-320 mimics/mimics NC and pEGFP-E2F1/pEGFP-SF-1/control vector into GCs. *K,* silencing of E2F-1 or SF-1 enhanced miR-320-induced proliferation suppression. Cell viability was analyzed after co-transfection with miR-320 mimics/control and 50 nM si-E2F1/si-SF-1/si.NC into GCs. *L* and *M,* miR-320 significantly attenuated SF-1-induced E_2 synthesis and rescued SF-1-mediated progesterone suppression in GCs. GCs were co-transfected with miR-320 mimics/mimics NC and pEGFP-SF-1/control vector. After 48 h of culture, media were collected for the measurement of E_2 (*L*) and progesterone (*M*) levels. *N* and *O,* changes in E2F1, SF-1, and CYP19A1 expression in ovaries of PMSG/hCG-treated immature mice. Total protein was extracted from ovaries of PMSG (20 IU)-treated mice at 0, 24, 48, or 72 h and PMSG/hCG-treated mice at indicated post-hCG time points and then subjected to Western blotting analysis (*N*). Representative Western blotting for SF-1 (*upper bands*), CYP19A1 (*upper middle bands*), E2F1 (*lower middle bands*), and actin (*lower bands*) (*N*) and the corresponding densitometric analysis (*O*) are shown. The ratio of the SF-1/CYP19A1/E2F1 band intensity over the actin band intensity in PMSG-untreated ovaries was arbitrarily set at 1.0. *P* and *Q,* E2F1 and SF-1 expression in ovaries of PND 1, 4, 10, 14, and 21 mice. Total protein was extracted from ovaries of PND 1, 4, 10, 14, and 21 mice and then subjected to Western blotting analysis (*P*). Representative Western blotting for SF-1 (*upper bands*), E2F1 (*middle bands*), and actin (*lower bands*) (*P*) and the corresponding densitometric analysis (*Q*) are shown. The ratio of the SF-1/E2F1 band intensity over the actin band intensity in PND 1 ovaries was arbitrarily set at 1.0. In *C–F, J–M, O* and *Q*, data represented the mean ± S.E. of three independent experiments performed in triplicate. *, $p < 0.05$; **, $p < 0.01$. +, present; −, absent.

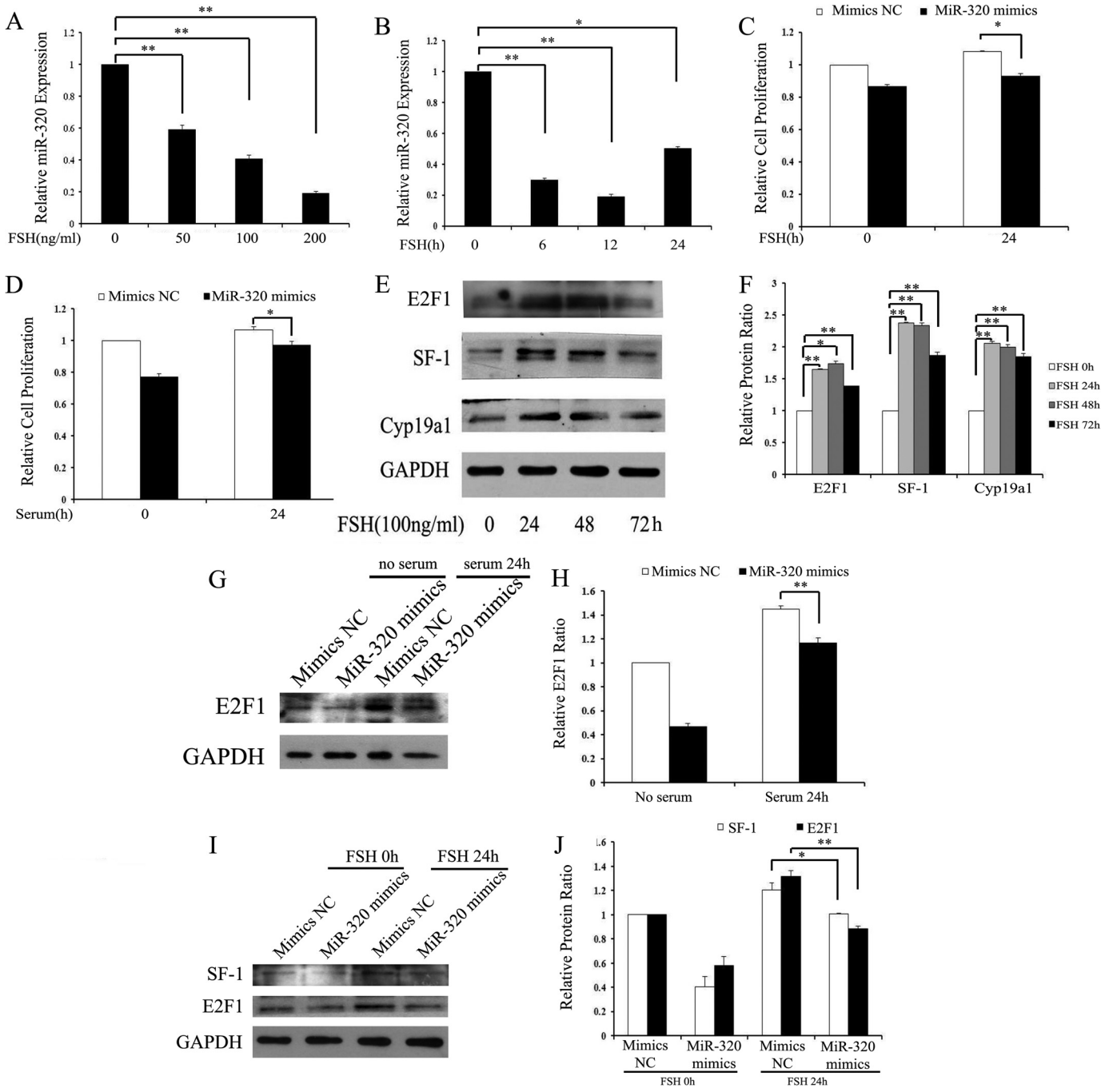

FIGURE 3. **FSH suppresses the expression of miR-320.** *A* and *B,* FSH repressed miR-320 expression. GCs were treated with FSH for the indicated time periods (*A*) and doses (*B*), and the expression levels of miR-320 were then examined by real time PCR analysis. *C* and *D*, miR-320 decreased GC proliferation induced by FSH (*C*) or serum (*D*). Cell viability was analyzed after transfection with miR-320 mimics/mimics NC and FSH/serum treatment/no treatment in GCs. *E* and *F*, FSH up-regulated E2F1 and SF-1 protein expression in mGCs. Cells were treated with 100 ng/ml FSH for the indicated time periods, and the expression levels of E2F1, SF-1, and CYP19A1 were then examined by Western blotting analysis (*E*). Representative Western blotting for E2F1 (*upper bands*), SF-1 (*upper middle bands*), CYP19A1 (*lower middle bands*), and GAPDH (*lower bands*) (*E*) and the corresponding densitometric analysis (*F*) are shown. The ratio of the SF-1/CYP19A1/E2F1 band intensity over the GAPDH band intensity in FSH untreatment was arbitrarily set at 1.0. *G* and *H*, overexpression of miR-320 inhibited serum-inducible E2F1 protein expression. Cells were transfected with the indicated oligonucleotides after serum starvation for 12 h. For Western blot analysis, cells were harvested 24 h after serum stimulation (*G*). Representative Western blotting for E2F1 (*upper bands*), and GAPDH (*lower bands*) (*G*) and the corresponding densitometric analysis (*H*) are shown. The ratio of the E2F1 band intensity over the GAPDH band intensity in Mimics NC/no serum treatment was arbitrarily set at 1.0. *I* and *J,* overexpression of miR-320 inhibited FSH-inducible E2F1 and SF-1 protein expression. Cells were transfected with the indicated oligonucleotides after serum starvation for 12 h. For Western blot analysis, cells were harvested 24 h after FSH treatment. Representative Western blotting for SF-1(*upper bands*), E2F1 (*middle bands*), and GAPDH (*lower bands*) (*I*) and the corresponding densitometric analysis (*J*) are shown. The ratio of the E2F1 band intensity over the GAPDH band intensity in Mimics NC/no serum treatment was arbitrarily set at 1.0. In *A–D, F, H,* and *J*, data represented the mean ± S.E. of three independent experiments performed in triplicate. *, $p < 0.05$; **, $p < 0.01$.

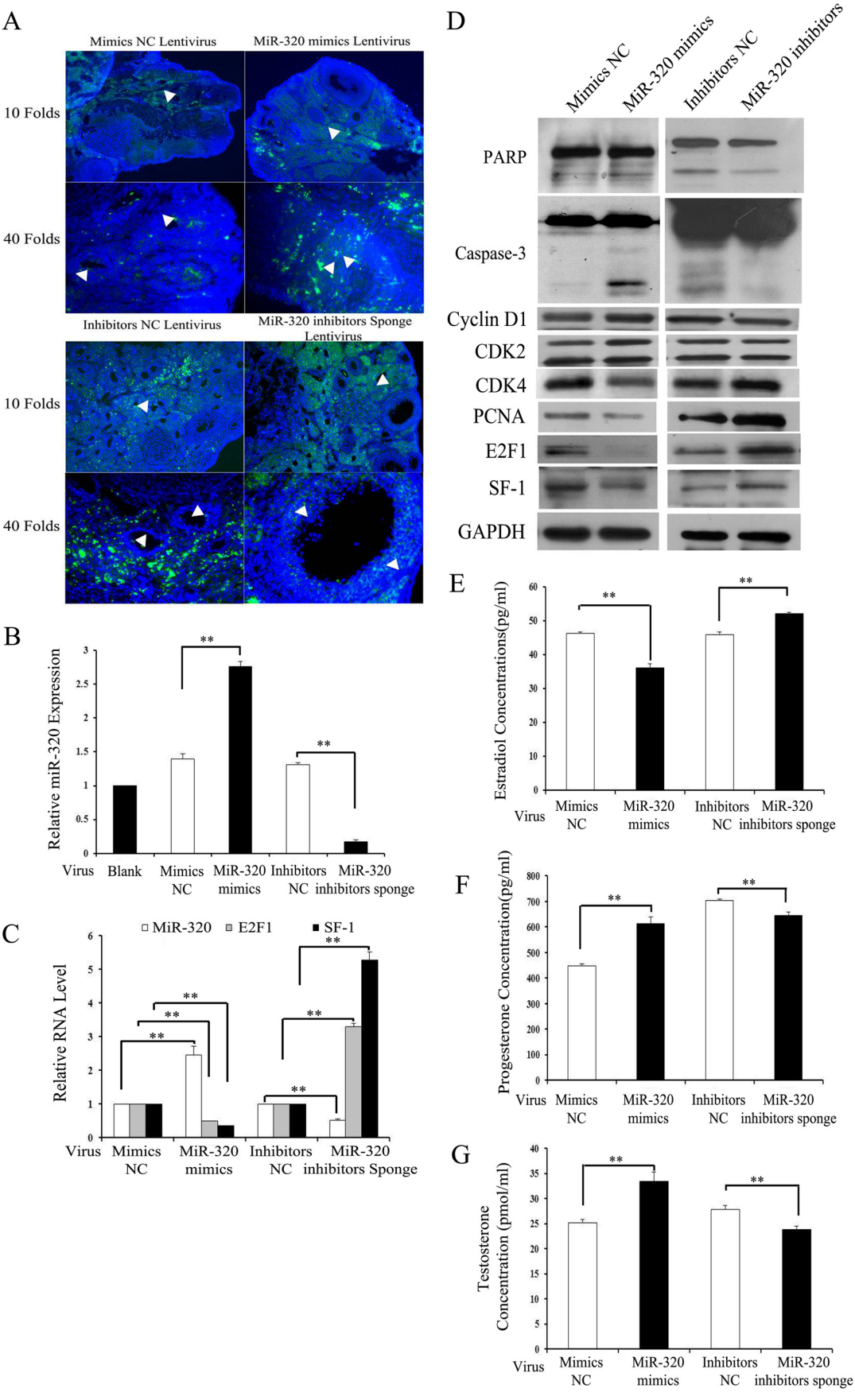
A
Mimics NC Lentivirus
MiR-320 mimics Lentivirus
10 Folds
40 Folds
Inhibitors NC Lentivirus
MiR-320 inhibitors Sponge Lentivirus
10 Folds
40 Folds
B
Relative miR-320 Expression
Virus Blank Mimics NC MiR-320 mimics Inhibitors NC MiR-320 inhibitors sponge
C
MiR-320 E2F1 SF-1
Relative RNA Level
Virus Mimics NC MiR-320 mimics Inhibitors NC MiR-320 inhibitors Sponge
D
Mimics NC
MiR-320 mimics
Inhibitors NC
MiR-320 inhibitors
PARP
Caspase-3
Cyclin D1
CDK2
CDK4
PCNA
E2F1
SF-1
GAPDH
E
Estradiol Concentrations(pg/ml)
Virus Mimics NC MiR-320 mimics Inhibitors NC MiR-320 inhibitors sponge
F
Progesterone Concentration(pg/ml)
Virus Mimics NC MiR-320 mimics Inhibitors NC MiR-320 inhibitors sponge
G
Testosterone Concentration (pmol/ml)
Virus Mimics NC MiR-320 mimics Inhibitors NC MiR-320 inhibitors sponge

miR-320 by miR-383, a series of deletion mutant constructs from −2941 to −48 nucleotides of the miR-320 promoter region were generated by cloning the relevant regions into the pGL3-Basic vector and transfecting them into HEK293T cells. Overexpression of miR-383 resulted in an ~1.5–2-fold increase in luciferase activities of almost all constructs compared with vector controls. Activities of miR-320 (−2019/−48) and miR-320 (−1282/−48) were higher than other deletion mutant constructs (Fig. 5*F*). These results indicate that the miR-320 promoter region from −999 to −2019 nucleotides might contain critical miR-383-responsive regulatory elements. Alignment analysis between miR-320 promoter and miR-383 revealed that there were three binding sites of miR-383 in the miR-320 promoter region from −2654 to −700 nucleotides (Fig. 5*G*). Forced expression of miR-383 failed to increase activity of the miR-320 promoter region (−2019/−48) containing mutations between −1124 and −1115 nucleotides (Fig. 5*H*). These results indicate that the miR-320 promoter region from −1124 to −1115 nucleotides might contain a critical miR-383-responsive regulatory element.

We next asked whether the target genes and functions of miR-320 were also regulated by miR-383. Immunoblotting results indicate that both miR-320 and miR-383 inhibited the expression of E2F1, whereas overexpression of miR-383 decreased the expression of E2F1 suppressed by miR-320 but did not change the expression of SF-1 suppressed by miR-320 (Fig. 5, *I* and *J*). Co-transfection of miR-383 mimics and miR-320 mimics into GCs resulted in a much greater decrease in cell proliferation (Fig. 5*K*) and rescued E_2 production suppressed by miR-320 mimics (Fig. 5*L*). An increase in E_2 production in GCs after co-transfection of miR-383 mimics and miR-320 mimics could be explained by increased expression of Cyp19a1 (Fig. 5*M*). These results demonstrated that miR-383 could enhance the effects of miR-320 on the target genes and cell proliferation.

Expression of miR-320 in the Follicular Fluid and GCs of Polycystic Ovaries—Because miR-320 not only significantly inhibits E_2 production but also induces progesterone and testosterone synthesis *in vivo* and *in vitro*, we examined whether miR-320 was involved in the reproductive or steroid-related disorders. We obtained the follicular fluid and GCs from normal controls, adenomyosis, endometriosis, endometrial polyps, and PCOS patients. The expression patterns of miR-383 and miR-320 were similar in different patients. The expression levels of miR-320 and miR-383 were lower in the follicular fluid of adenomyosis and endometriosis patients, as compared with the follicular fluid of normal controls (Fig. 6, *A* and *B*). There was no difference in the miR-383 and miR-320 expression level between endometrial polyps and normal controls, whereas the expression levels of miR-383 and miR-320 were higher in the follicular fluid (Fig. 6, *A* and *B*) and GCs (Fig. 6, *C* and *D*) of PCOS patients than that in normal controls. Hyperandrogenemia is the major marker of the polycystic ovarian morphology (Fig. 6, *E* and *F*) (47). The real time PCR results showed that the expression levels of E2F1 and SF-1 in the follicular fluid (Fig. 6, *G* and *H*) and GCs (Fig. 6, *I* and *J*) of PCOS patients were lower than that in normal controls. These results verify that miR-320 regulates, at least in part, the expression and functions of E2F1 and SF-1 in PCOS patients.

DISCUSSION

In this study, we have found that miR-320 not only significantly decelerates cell proliferation and E_2 production but also promotes progesterone synthesis in mGCs by directly targeting E2F1 and SF-1 *in vivo* and *in vitro*. miR-383 activates the expression of miR-320 through binding to a potential miR-383 response element in the miR-320 promoter and enhances the effects of miR-320 on cell proliferation through inhibiting the expression of E2F1 in GCs. The expression of miR-320 was higher in the follicular fluid and GCs of PCOS patients than that in normal controls, whereas E2F1 and SF-1 expression correlated negatively with the miR-320 expression in the follicular fluid and GCs of PCOS patients. Here, we provide mechanistic insights into the role of miR-320 in ovarian follicle development and reveal a new mechanism for PCOS.

Gonadal steroid hormones and cell proliferation play critical roles in normal reproductive processes (48–50) as well as in the development of some reproductive and nonreproductive pathology, including PCOS (51), and estrogen-related cancer (52) in women. Thus, a deeper understanding of the molecular mechanisms controlling steroid production and cell proliferation within GCs may help the potential application of miRNAs in the control of reproduction and the treatment of some reproductive and steroid-related disorders. miRNA populations have been identified by next-generation or cloning-based sequencing of normal ovarian tissues from humans (25) and mice (26, 53, 54). Lists of miRNAs expressed in specific ovarian compartments, including follicular GCs (14), corpora lutea (55), cumulus-oocyte complexes (56), and follicular fluid (57), have been identified using mouse- or human-based microarrays or high throughput real time PCR. miR-378 was shown to suppress estradiol production by directly targeting aromatase in porcine GCs (13). Yang *et al.* (58) reported that miR-23a was pro-apoptotic in cultured human luteinized granulosa cells, presumably by increasing caspase-3 cleavage and suppressing the levels of X-linked inhibitor of apoptosis protein. In our previous study, we found that miR-224 promotes TGF-β1-induced mGC E_2 production by targeting Smad4 (14), whereas miRNA-383 increases estradiol release from mouse ovarian GCs by targeting RBMS1 (15). miR-320 was the second most down-regulated miRNA in mGCs treated with TGF-β1 (14). In this study,

FIGURE 4. **miR-320 regulates the expression of E2F1/SF-1 and GC function *in vivo*.** *A,* localization of GFP-labeled miR-320 mimics/mimics NC and miR-320 inhibitors sponge/inhibitors NC lentivirus in the ovaries was examined under a fluorescent microscope with Hoechst staining. *Arrows* indicate the lentivirus in the GCs of the ovary. *B* and *C*, infection efficiency of miR-320 mimics and miR-320 inhibitors sponge virus in GCs (*B*) and ovaries of mice (*C*) was determined by real time PCR. Total RNA was extracted from ovaries/GCs and then subjected to analysis to the expression of miR-320, E2f-1, and Sf-1 (*C*). *D,* miR-320 regulated the expression of SF-1, E2F1, PCNA, CDK4, CDK2, cyclin D1, caspase-3, and PARP in the ovaries *in vivo*. Ovaries were infected with lentivirus for 3 days as described above. Expression of SF-1, E2F1, PCNA, CDK4, CDK2, cyclin D1, caspase-3, and PARP in the ovaries was determined by Western blotting. *E–G,* miR-320 affected steroidogenesis *in vivo*. Ovaries were infected with lentivirus for 3 days as described above. Sera of the mice were collected for measurement of E_2 (*E*), progesterone (*F*), and testosterone (*G*) levels. *B* and *C* and *E–G,* data represented the mean ± S.E. of three independent experiments performed in triplicate. **, $p < 0.01$.

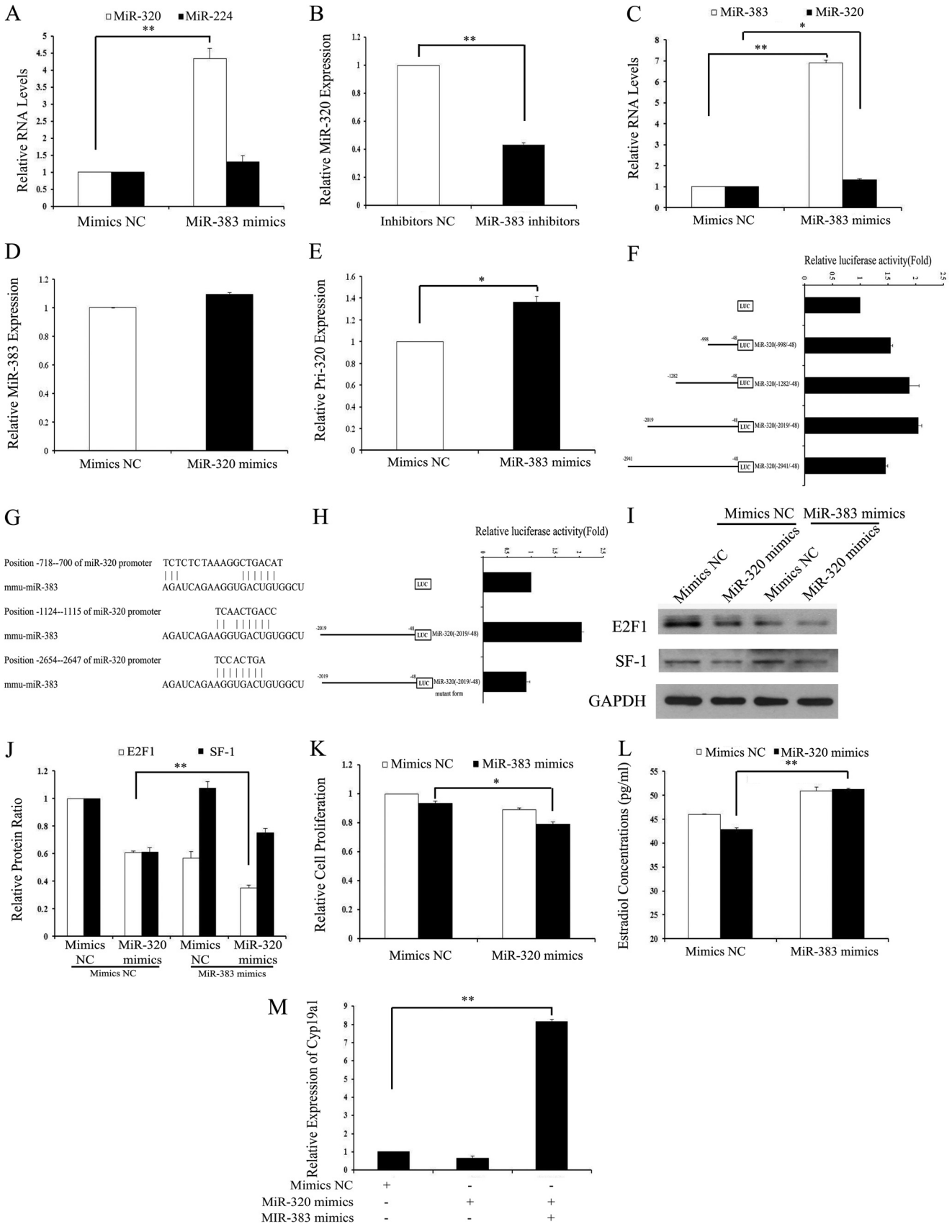
A
MiR-320
MiR-224
Relative RNA Levels
Mimics NC
MiR-383 mimics
B
Relative MiR-320 Expression
Inhibitors NC
MiR-383 inhibitors
C
MiR-383
MiR-320
Relative RNA Levels
Mimics NC
MiR-383 mimics
D
Relative MiR-383 Expression
Mimics NC
MiR-320 mimics
E
Relative Pri-320 Expression
Mimics NC
MiR-383 mimics
F
Relative luciferase activity(Fold)
LUC
MiR-320(-998/-48)
MiR-320(-1282/-48)
MiR-320(-2019/-48)
MiR-320(-2941/-48)
G
Position -718--700 of miR-320 promoter TCTCTCTAAAGGCTGACAT
mmu-miR-383 AGAUCAGAAGGUGACUGUGGCU
Position -1124--1115 of miR-320 promoter TCAACTGACC
mmu-miR-383 AGAUCAGAAGGUGACUGUGGCU
Position -2654--2647 of miR-320 promoter TCCACTGA
mmu-miR-383 AGAUCAGAAGGUGACUGUGGCU
H
Relative luciferase activity(Fold)
LUC
MiR-320(-2019/-48)
MiR-320(-2019/-48) mutant form
I
Mimics NC
MiR-383 mimics
Mimics NC
MiR-320 mimics
Mimics NC
MiR-320 mimics
E2F1
SF-1
GAPDH
J
E2F1
SF-1
Relative Protein Ratio
Mimics NC
MiR-320 mimics
Mimics NC
MiR-320 mimics
Mimics NC
MiR-383 mimics
K
Mimics NC
MiR-383 mimics
Relative Cell Proliferation
Mimics NC
MiR-320 mimics
L
Mimics NC
MiR-320 mimics
Estradiol Concentrations (pg/ml)
Mimics NC
MiR-383 mimics
M
Relative Expression of Cyp19a1
Mimics NC + - -
MiR-320 mimics - + +
MIR-383 mimics - - +

we found that miR-320, which was expressed mainly in GCs of follicles at different developmental stages, not only inhibited E_2 release and cell proliferation in mGCs but also enhanced progesterone synthesis in mGCs *in vivo* and *in vitro*. In addition, we found a negative correlation between the pattern of miR-320 expression and the pattern of serum E_2 and GC proliferation in PMSG-treated immature female mice. miR-320 expression in isolated mouse follicles decreased from the pre-antral to antral phase. These results indicate that miR-320 might exert effects on GC proliferation and steroidogenesis by regulating proliferation- or steroidogenesis-associated genes during follicular development. Here, our studies add miR-320 as another potent regulator of ovarian functions.

miRNAs are shown to result in diverse biological outcomes through regulating genes involved in normal development and pathological responses (59–61). miR-320 has been reported to play different roles by regulating genes in several biological processes. For example, PTEN-regulated miR-320 acts in stromal fibroblasts to reprogram the tumor microenvironment and curtail tumor progression (62); miR-320 increases neurite length by targeting ARPP-19 (32); miR-320 negatively regulates expression of ET-1, VEGF, and fibronectin through ERK1/2 in diabetes (63); miR-320 and miR-702 increase the proliferation of Dgcr8-deficient embryonic stem cells by inhibiting p57 and p21 expression (31); and overexpression of miR-320 decreases prostate cancer tumorigenesis by down-regulating the Wnt/β-catenin signaling pathway *in vitro* and i*n vivo* (64). However, the functions and expression of miR-320 in ovarian GCs have not been studied. In this study, miR-320 regulated the GC proliferation and steroidogenesis by directly targeting E2F1 and SF-1. E2F1 has been shown to regulate the cell cycle by binding preferentially to retinoblastoma protein pRB and mediates both p53-dependent/independent apoptosis and cell proliferation (9, 10). miR-E2F1 interactions might contribute either to the oncogenic or to the tumor-suppressive functions of E2F1 (65). The miR-106b∼25 and miR-17∼92 cluster suppress excessively high E2F1 expression that may otherwise result in tumor cell apoptosis (59, 66). miR-106a (67), miR-330-3p (68), miR-34 family (69), miR-223 (70), miR-15 family (71), and miR-205 (72) have been shown to act as tumor suppressors through negative regulation of E2F1 expression in cancer cells. SF-1 plays an important role in the development and differentiation of steroidogenic tissues (73). miR-23a and miR-23b deregulation inhibits SF-1 and enhances estrogen signaling in ovarian endometriosis (74). Because miRs themselves are transcriptionally regulated by RNA polymerase II, they can also be regulated by some transcription factors. Some miRs are not only important modulators of E2F1 expression but are also controlled by the E2F1 transcription factor in an autoregulatory feedback loop. E2F1 directly binds to the promoter of the miR-17∼92 cluster and activates its transcription, whereas miRs encoded by E2F1 in turn negatively regulate expression of E2F1 via binding sites in its 3′UTR (75). E2F1 transactivates miR-449, which enhances the p53 pathway, thereby promoting the expression of miR-34. In turn, miR-449 and miR-34 inhibit the E2F pathway in a negative feedback loop and result in growth arrest (76). Transactivation of miR-383 by SF-1 binding to the promoter of *SGCZ* increases E_2 production in mouse ovarian GCs (15). In this study, E2F1 and SF-1 were also mainly located in GCs of various follicle stages. Knockdown of E2F1 and SF-1 in GCs inhibited GC proliferation. In addition, E2F1/SF-1 mediated the effect of miR-320 on GC proliferation. These results indicate that E2F1 and SF-1 function as potent regulators of GC proliferation during ovarian development. Although we used E2F1 and SF-1 to determine the role of miR-320 in ovarian development, other miRNA-regulated proteins may also participate in ovarian development, and thus, other unknown miRNAs may also be important in ovarian functioning. Several miRNAs have been implicated in the control of various proliferation and steroidogenesis-related molecules and thus may positively or negatively affect proliferation and steroidogenesis in a system-dependent manner. Whether miRNAs are commonly involved in proliferation and steroidogenesis in the ovary and other systems needs further investigation. Whether miR-320 targets the homologs of the *E2f1*/*Sf-1* gene and participates in the processes attributable to E2F1/SF-1, such as proliferation and apoptosis, and E2F1/SF-1 transactivates some miRNA expression, remains to be elucidated.

The initial trigger of immature pre-antral follicle development to a pre-ovulatory follicle is FSH stimulation of GC differentiation (77). FSH regulates the development of GCs during folliculogenesis by enhancing their differentiation and prolifer-

FIGURE 5. **miR-383 promotes the expression of miR-320 in GCs.** *A* and *B,* miR-383 regulated the miR-320 levels. GCs were transfected with 120 nM miR-383 mimics/mimics NC (*A*) or 150 nM miR-383 inhibitors/inhibitors NC (*B*), and then the levels of miR-320 and miR-224 were determined after 48 h of transfection by real time PCR. *C,* miR-383 regulated the expression of miR-320 in the ovaries *in vivo*. Ovaries were injected with miR-383 mimics for 3 days as described above. Expression of miR-383 and miR-320 in the ovaries was determined by real time PCR. *D,* miR-320 had no effect on the expression of miR-383. GCs were transfected with 120 nM miR-320 mimics/mimics NC, and then the levels of miR-383 were determined after 48 h of transfection by real time PCR. *E,* miR-383 regulated the levels of primary miR-320. GCs were transfected with 120 nM miR-383 mimics/mimics NC, and then the level of primary miR-320 was determined after 48 h of transfection by real time PCR. *F,* identification of the minimal promoter region of miR-320. *Left panel,* schematic representation of 5′- or 3′-deleted fragments of miR-320 promoter in conjunction with the luciferase gene (*LUC*) in a pGL3-Basic vector. The nucleotides are numbered from the transcriptional starting site. *Right panel,* luciferase activities of the deleted miR-320 promoter constructs. HEK293T cells were co-transfected with miR-383 mimics and serial mouse miR-320 promoter-luciferase reporter deletion constructs. Relative promoter luciferase activity was calculated as a ratio of luciferase activity of the miR-320 promoter deletion constructs driven by miR-383 over the pGL3-Basic empty vector, which was arbitrarily set at 1. *G,* putative-binding sites for mmu-miR-383 are predicted in the 3000 bp of the miR-320 promoter. *H,* mutational analysis of miR-320 promoter-luciferase reporter constructs. miR-320 promoter regions (−2019/−48) containing mutations between −1124 and −1115 nucleotides were cloned into the luciferase reporter vector pGL3-Basic. *I–K,* overexpression of miR-383 enhanced miR-320-induced inhibition of E2F1 expression and proliferation suppression. The protein expression of E2F1/SF-1 (*I* and *J*) and cell viability (*K*) was analyzed after co-transfection with miR-320 mimics/mimics NC and miR-383 mimics/mimics NC into GCs. Representative Western blotting for E2F1 (*upper bands*), SF-1 (*middle bands*), and GAPDH (*lower bands*) (*I*) and the corresponding densitometric analysis (*J*) are shown. The ratio of the E2F1 band intensity over the GAPDH band intensity in controls was arbitrarily set at 1.0. *L,* overexpression of miR-383 rescued miR-320-induced E_2 suppression. E_2 were measured after co-transfection with miR-320 mimics/mimics NC and miR-383 mimics/mimics NC into GCs. *M,* overexpression of miR-383 rescued miR-320-induced suppression of CYP19A1 expression. The mRNA of *Cyp19a1* was measured after co-transfection with miR-320 mimics/mimics NC and miR-383 mimics/mimics NC into GCs by real time PCR. *A–F, H,* and *J–M,* data represent the mean ± S.E. of three independent experiments performed in triplicate. *, $p < 0.05$; **, $p < 0.01$.

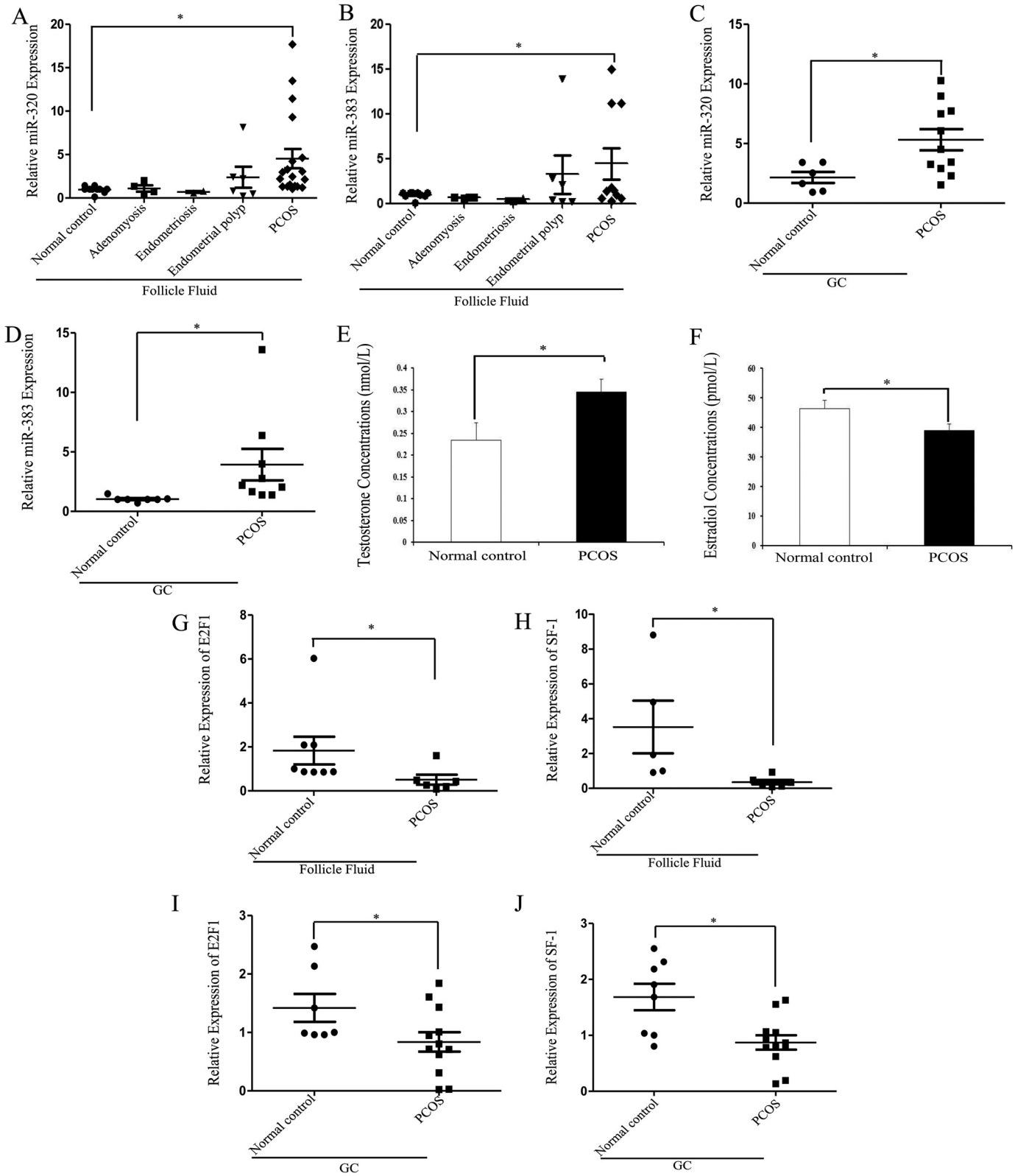

FIGURE 6. **Up-regulation of miR-320 expression in PCOS patients.** *A* and *B*, expressions of miR-320 and miR-383 in the follicular fluid from normal controls, adenomyosis, endometriosis, endometrial polyps, and PCOS patients were determined by real time PCR in triplicate. *C* and *D*, expressions of miR-320 (*C*) and miR-383 (*D*) in the GCs from normal controls and PCOS patients were determined by real time PCR in triplicate. *E* and *F*, concentrations of testosterone (*E*) and estradiol (*F*) in the normal controls and PCOS patients. *G–J*, expressions of *E2F1* and *SF-1* in the follicular fluid (*G* and *H*) and GCs (*I* and *J*) from normal controls and PCOS patients were determined by real time PCR in triplicate. *, $p < 0.05$.

ation, and by promoting the formation of the follicular antrum (78). FSH transcriptionally controls multiple GC genes during FSH-induced proliferation and steroidogenesis, including CYP19A1 (79) and bone morphogenetic proteins (80). Yao *et al.* (81) have shown that the expression of 31 miRNAs is regulated during FSH-mediated progesterone synthesis of cultured rat granulosa cells. Additionally, they have examined the expression of miR-29a and miR-30d to be significantly down-regulated by FSH, and have analyzed their potential targets (81). Although miRNAs have been reported in FSH treatment in rat GCs, the effect of FSH on the regulation of miRNAs in mouse GCs is still unclear. In this study, the expression of miR-320 was suppressed during FSH treatment, whereas miR-320 suppressed the expression of E2F1, SF-1, and CYP19A1. These results indicate that FSH might induce the expression of E2F1, SF-1, and CYP19A1 by inhibiting the expression of miR-320. Further studies will be required to more precisely determine the modulation of FSH in miR-320, E2F1, SF-1, and CYP19A1 expression. In particular, FSH induces the secretion of the female sex hormones estradiol and progesterone, which control the differentiation of GCs and reproduction (81). miR-320 mediates the effect of FSH on the GC proliferation, but whether miR-320 is commonly involved in FSH-induced estradiol and progesterone synthesis in GCs requires further investigation. It should be noted that our results do not exclude the possibility that the expression of other miRNAs and their target genes were also altered in FSH-treated GCs. Taken together, our studies reveal new insights into the mechanism of FSH action.

The injection of miR-320 mimics lentivirus into the ovarian bursa of mice partially inhibited cell proliferation and E_2 secretion and increased the production of progesterone and testosterone. Up-regulated testosterone secretion might be the reason for impaired E_2 production in the miR-320-treated mice. Transformation of androgens into estrogens might be interfered with proteins or small molecules that were regulated by miR-320 *in vivo*. We also detected the apoptosis signal in the stromal cells, which might indicate that miR-320 not only promotes the apoptosis of GCs but also increases the apoptosis of stromal cells in the ovary. Ovarian theca cells are the main source of androgen. Whether miR-320 controls the production of androgen in the cultured theca cells requires further investigation. Androgens were shown to increase apoptosis, and estrogens revealed a protective trend on cell death (43). Increased progesterone secretion might be a partial cause of apoptosis in the ovaries injected with miR-320 lentivirus. It should be noted that our results do not exclude the possibility that other apoptosis-related genes were regulated by miR-320.

Our previous studies have shown that miR-383 and miR-320 are two of the most down-regulated miRNAs, and miR-224 is the second most significantly elevated miRNA in TGF-β1-treated mouse ovarian GCs (14, 15). These results indicate that they might interact with each other in mGCs. Indeed, miR-383 promoted the expression of miR-320 by binding to the promoter of miR-320, whereas miR-320 did not affect the expression of miR-383. However, further studies will be required to more precisely determine the modulation of miR-383 in miR-320 processing through site-directed mutagenesis and deletion analysis. Whether both miR-383 and miR-320 are regulated by the same transcription factor or target genes of miR-383 down-regulated the expression of miR-320 in the ovary systems requires further investigation.

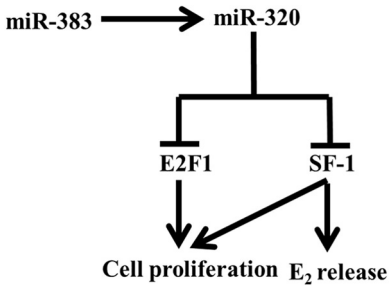

FIGURE 7. **Model for the pathway through miR-383-mediated transcription of miR-320 in GCs.** Transactivation of miR-320 by miR-383 inhibits the expression of E2F1 and SF-1 and subsequently inhibits E_2 release and cell proliferation in GCs.

In this study, high levels of miR-320 and hyperandrogenemia and down-regulation of E2F1/SF-1 were observed in the follicular fluid and GCs of PCOS patients. In addition, miR-320 increases testosterone secretion *in vivo*. These results indicate that high levels of miR-320 may be the partial reason for hyperandrogenemia in PCOS patients. These effects of miR-320 on physiological processes within the ovary suggest the potential usefulness of miR-320 in the control of reproduction and treatment of some reproductive and steroid-related disorders. For example, miR-320, which increases an endogenous progesterone surge, could be used in addition to or instead of its analogs or native progesterone, which are currently widely used as contraceptive pills in reproductive medicine and family planning. miR-320 inhibitors suppressing testosterone production could be tested for the inhibition of testosterone overproduction, which is the main cause of PCOS.

In summary, we demonstrate that miR-320 functions as a negative regulator of E_2 release and cell proliferation and a positive regulator of progesterone in GCs through inhibiting expression of E2F1 and SF-1 *in vivo* and *in vitro*. Moreover, miR-383 increases the expression of miR-320 and enhances its effect on cell proliferation (Fig. 7). The mechanistic studies regarding the role of miR-320 in PCOS will provide new clues to treating PCOS. It should be noted that our results do not exclude the possibility that other ovarian functions, such as folliculogenesis, oocyte maturation, and ovulation, are regulated by miR-320. However, our results showed that GC proliferation and steroidogenesis of the ovary is the physiological process that appears to be most sensitive to miR-320 during ovary development. This study demonstrates that miR-320 could be involved in the cell proliferation and steroidogenesis and may have therapeutic implications not only for the control of fertility but also for the treatment of steroid disorders and other pathological conditions characterized by abnormal cell proliferation and steroidogenesis in the ovary.

Acknowledgments—We thank Dr. Mian Wu and Dr. Tao Zhu (Hefei, China) for the HEK293T and MCF-7 cell lines.

REFERENCES

1. Nelson, L. R., and Bulun, S. E. (2001) Estrogen production and action. *J. Am. Acad. Dermatol.* **45,** S116–124

2. Jamnongjit, M., Gill, A., and Hammes, S. R. (2005) Epidermal growth factor receptor signaling is required for normal ovarian steroidogenesis and oocyte maturation. *Proc. Natl. Acad. Sci. U.S.A.* **102,** 16257–16262
3. Gallo, R. V. (1981) Pulsatile LH release during the ovulatory LH surge on proestrus in the rat. *Biol. Reprod.* **24,** 100–104
4. Parakh, T. N., Hernandez, J. A., Grammer, J. C., Weck, J., Hunzicker-Dunn, M., Zeleznik, A. J., and Nilson, J. H. (2006) Follicle-stimulating hormone/cAMP regulation of aromatase gene expression requires β-catenin. *Proc. Natl. Acad. Sci. U.S.A.* **103,** 12435–12440
5. Michael, M. D., Kilgore, M. W., Morohashi, K., and Simpson, E. R. (1995) Ad4BP/SF-1 regulates cyclic AMP-induced transcription from the proximal promoter (PII) of the human aromatase P450 (CYP19) gene in the ovary. *J. Biol. Chem.* **270,** 13561–13566
6. Jeyasuria, P., Ikeda, Y., Jamin, S. P., Zhao, L., De Rooij, D. G., Themmen, A. P., Behringer, R. R., and Parker, K. L. (2004) Cell-specific knockout of steroidogenic factor 1 reveals its essential roles in gonadal function. *Mol. Endocrinol.* **18,** 1610–1619
7. Berkovich, E., and Ginsberg, D. (2003) ATM is a target for positive regulation by E2F-1. *Oncogene* **22,** 161–167
8. Crosby, M. E., and Almasan, A. (2004) Opposing roles of E2Fs in cell proliferation and death. *Cancer Biol. Ther.* **3,** 1208–1211
9. Qin, X. Q., Livingston, D. M., Kaelin, W. G., Jr., and Adams, P. D. (1994) Deregulated transcription factor E2f-1 expression leads to S-phase entry and P53-mediated apoptosis. *Proc. Natl. Acad. Sci. U.S.A.* **91,** 10918-10922
10. Holmberg, C., Helin, K., Sehested, M., and Karlström, O. (1998) E2F-1-induced p53-independent apoptosis in transgenic mice. *Oncogene* **17,** 143–155
11. Lee, K. H., Sburlati, A., Renner, W. A., and Bailey, J. E. (1996) Deregulated expression of cloned transcription factor E2F-1 in Chinese hamster ovary cells shifts protein patterns and activates growth in protein-free medium. *Biotechnol. Bioeng.* **50,** 273–279
12. Majors, B. S., Arden, N., Oyler, G. A., Chiang, G. G., Pederson, N. E., and Betenbaugh, M. J. (2008) E2F-1 overexpression increases viable cell density in batch cultures of Chinese hamster ovary cells. *J. Biotechnol.* **138,** 103–106
13. Xu, S., Linher-Melville, K., Yang, B. B., Wu, D., and Li, J. (2011) Micro-RNA378 (miR-378) Regulates ovarian estradiol production by targeting aromatase. *Endocrinology* **152,** 3941–3951
14. Yao, G., Yin, M., Lian, J., Tian, H., Liu, L., Li, X., and Sun, F. (2010) MicroRNA-224 is involved in transforming growth factor-β-mediated mouse granulosa cell proliferation and granulosa cell function by targeting smad4. *Mol. Endocrinol.* **24,** 540–551
15. Yin, M., Lü, M., Yao, G., Tian, H., Lian, J., Liu, L., Liang, M., Wang, Y., and Sun, F. (2012) Transactivation of microRNA-383 by steroidogenic factor-1 promotes estradiol release from mouse ovarian granulosa cells by targeting RBMS1. *Mol. Endocrinol.* **26,** 1129–1143
16. Fire, A., Xu, S., Montgomery, M. K., Kostas, S. A., Driver, S. E., and Mello, C. C. (1998) Potent and specific genetic interference by double-stranded RNA in *Caenorhabditis elegans*. *Nature* **391,** 806–811
17. Stefani, G., and Slack, F. (2006) MicroRNAs in search of a target. *Cold Spring Harbor Symp. Quant. Biol.* **71,** 129–134
18. Yang, M., and Mattes, J. (2008) Discovery, biology and therapeutic potential of RNA interference, microRNA, and antagomirs. *Pharmacol. Ther.* **117,** 94–104
19. Cheng, A. M., Byrom, M. W., Shelton, J., and Ford, L. P. (2005) Antisense inhibition of human miRNAs and indications for an involvement of miRNA in cell growth and apoptosis. *Nucleic Acids Res.* **33,** 1290–1297
20. Lei, L., Jin, S., Gonzalez, G., Behringer, R. R., and Woodruff, T. K. (2010) The regulatory role of Dicer in folliculogenesis in mice. *Mol. Cell. Endocrinol.* **315,** 63–73
21. Murchison, E. P., Stein, P., Xuan, Z., Pan, H., Zhang, M. Q., Schultz, R. M., and Hannon, G. J. (2007) Critical roles for Dicer in the female germline. *Gene Dev.* **21,** 682–693
22. Otsuka, M., Zheng, M., Hayashi, M., Lee, J. D., Yoshino, O., Lin, S., and Han, J. (2008) Impaired microRNA processing causes corpus luteum insufficiency and infertility in mice. *J. Clin. Investig.* **118,** 1944–1954
23. Hong, X., Luense, L. J., McGinnis, L. K., Nothnick, W. B., and Christenson, L. K. (2008) Dicer1 is essential for female fertility and normal development of the female reproductive system. *Endocrinology* **149,** 6207–6212
24. Nagaraja, A. K., Andreu-Vieyra, C., Franco, H. L., Ma, L., Chen, R., Han, D. Y., Zhu, H., Agno, J. E., Gunaratne, P. H., DeMayo, F. J., and Matzuk, M. M. (2008) Deletion of Dicer in somatic cells of the female reproductive tract causes sterility. *Mol. Endocrinol.* **22,** 2336–2352
25. Landgraf, P., Rusu, M., Sheridan, R., Sewer, A., Iovino, N., Aravin, A., Pfeffer, S., Rice, A., Kamphorst, A. O., Landthaler, M., Lin, C., Socci, N. D., Hermida, L., Fulci, V., Chiaretti, S., Foà, R., Schliwka, J., Fuchs, U., Novosel, A., Müller, R. U., Schermer, B., Bissels, U., Inman, J., Phan, Q., Chien, M., Weir, D. B., Choksi, R., De Vita, G., Frezzetti, D., Trompeter, H. I., Hornung, V., Teng, G., Hartmann, G., Palkovits, M., Di Lauro, R., Wernet, P., Macino, G., Rogler, C. E., Nagle, J. W., Ju, J., Papavasiliou, F. N., Benzing, T., Lichter, P., Tam, W., Brownstein, M. J., Bosio, A., Borkhardt, A., Russo, J. J., Sander, C., Zavolan, M., and Tuschl, T. (2007) A mammalian microRNA expression atlas based on small RNA library sequencing. *Cell* **129,** 1401–1414
26. Ro, S., Song, R., Park, C., Zheng, H., Sanders, K. M., and Yan, W. (2007) Cloning and expression profiling of small RNAs expressed in the mouse ovary. *RNA* **13,** 2366–2380
27. Li, M., Liu, Y., Wang, T., Guan, J., Luo, Z., Chen, H., Wang, X., Chen, L., Ma, J., Mu, Z., Jiang, A. A., Zhu, L., Lang, Q., Zhou, X., Wang, J., Zeng, W., Li, N., Li, K., Gao, X., and Li, X. (2011) Repertoire of porcine microRNAs in adult ovary and testis by deep sequencing. *Int. J. Biol. Sci.* **7,** 1045–1055
28. Corney, D. C., Flesken-Nikitin, A., Godwin, A. K., Wang, W., and Nikitin, A. Y. (2007) MicroRNA-34b and microRNA-34c are targets of p53 and cooperate in control of cell proliferation and adhesion-independent growth. *Cancer Res.* **67,** 8433–8438
29. Moore, R. K., and Shimasaki, S. (2005) Molecular biology and physiological role of the oocyte factor, BMP-15. *Mol. Cell. Endocrinol.* **234,** 67–73
30. Mondschein, J. S., Canning, S. F., and Hammond, J. M. (1988) Effects of transforming growth factor-β on the production of immunoreactive insulin-like growth factor-I and progesterone and on [^{3}H]thymidine incorporation in porcine granulosa-cell cultures. *Endocrinology* **123,** 1970-1976
31. Kim, B. M., and Choi, M. Y. (2012) Non-canonical microRNAs miR-320 and miR-702 promote proliferation in Dgcr8-deficient embryonic stem cells. *Biochem. Biophys. Res. Commun.* **426,** 183–189
32. White, R. E., and Giffard, R. G. (2012) MicroRNA-320 induces neurite outgrowth by targeting ARPP-1. *Neuroreport* **23,** 590–595
33. Willis, D. S., Watson, H., Mason, H. D., Galea, R., Brincat, M., and Franks, S. (1998) Premature response to luteinizing hormone of granulosa cells from anovulatory women with polycystic ovary syndrome: Relevance to mechanism of anovulation. *J. Clin. Endocr. Metab.* **83,** 3984–3991
34. Robinson, S., Kiddy, D., Gelding, S. V., Willis, D., Niththyananthan, R., Bush, A., Johnston, D. G., and Franks, S. (1993) The relationship of insulin insensitivity to menstrual pattern in women with hyperandrogenism and polycystic ovaries. *Clin. Endocrinol.* **39,** 351–355
35. Gilling-Smith, C., Willis, D. S., Beard, R. W., and Franks, S. (1994) Hypersecretion of androstenedione by isolated thecal cells from polycystic ovaries. *J. Clin. Endocr. Metab.* **79,** 1158–1165
36. Gilling-Smith, C., Story, H., Rogers, V., and Franks, S. (1997) Evidence for a primary abnormality of thecal cell steroidogenesis in the polycystic ovary syndrome. *Clin. Endocrinol.* **47,** 93–99
37. Nielsen, M. E., Rasmussen, I. A., Kristensen, S. G., Christensen, S. T., Møllgård, K., Wreford Andersen, E., Byskov, A. G., and Yding Andersen, C. (2011) In human granulosa cells from small antral follicles, androgen receptor mRNA and androgen levels in follicular fluid correlate with FSH receptor mRNA. *Mol. Hum. Reprod.* **17,** 63–70
38. Lian, J., Tian, H., Liu, L., Zhang, X. S., Li, W. Q., Deng, Y. M., Yao, G. D., Yin, M. M., and Sun, F. (2010) Downregulation of microRNA-383 is associated with male infertility and promotes testicular embryonal carcinoma cell proliferation by targeting IRF1. *Cell Death Dis.* **1,** e94
39. Shao, R., Ljungström, K., Weijdegård, B., Egecioglu, E., Fernandez-Rodriguez, J., Zhang, F. P., Thurin-Kjellberg, A., Bergh, C., and Billig, H. (2007) Estrogen-induced upregulation of AR expression and enhancement of AR nuclear translocation in mouse fallopian tubes *in vivo*. *Am. J. Physiol. Endocrinol. Metab.* **292,** E604–E614

40. Vanderhyden, B. C., Cohen, J. N., and Morley, P. (1993) Mouse oocytes regulate granulosa-cell steroidogenesis. *Endocrinology* **133,** 423–426
41. Vitt, U. A., Kloosterboer, H. J., Rose, U. M., Mulders, J. W., Kiesel, P. S., Bete, S., and Nayudu, P. L. (1998) Isoforms of human recombinant follicle-stimulating hormone: comparison of effects on murine follicle development *in vitro*. *Biol. Reprod.* **59,** 854–861
42. Boulares, A. H., Yakovlev, A. G., Ivanova, V., Stoica, B. A., Wang, G., Iyer, S., and Smulson, M. (1999) Role of poly(ADP-ribose) polymerase (PARP) cleavage in apoptosis- caspase 3-resistant PARP mutant increases rates of apoptosis in transfected cells. *J. Biol. Chem.* **274,** 22932–22940
43. Cutolo, M., Capellino, S., Montagna, P., Ghiorzo, P., Sulli, A., and Villaggio, B. (2005) Sex hormone modulation of cell growth and apoptosis of the human monocytic/macrophage cell line. *Arthritis Res. Ther.* **7,** R1124-1132
44. Wang, W., Chen, X., Li, X., Wang, L., Zhang, H., He, Y., Wang, J., Zhao, Y., Zhang, B., and Xu, Y. (2011) Interference RNA-based silencing of endogenous SMAD4 in porcine granulosa cells resulted in decreased FSH-mediated granulosa cells proliferation and steroidogenesis. *Reproduction* **141,** 643–651
45. Hunzicker-Dunn, M., and Maizels, E. T. (2006) FSH signaling pathways in immature granulosa cells that regulate target gene expression: branching out from protein kinase A. *Cell. Signal.* **18,** 1351–1359
46. Kim, V. N. (2005) MicroRNA biogenesis: coordinated cropping and dicing. *Nat. Rev. Mol. Cell Biol.* **6,** 376–385
47. Webber, L. J., Stubbs, S., Stark, J., Trew, G. H., Margara, R., Hardy, K., and Franks, S. (2003) Formation and early development of follicles in the polycystic ovary. *Lancet* **362,** 1017–1021
48. Hillier, S. G. (2001) Gonadotropic control of ovarian follicular growth and development. *Mol. Cell. Endocrinol.* **179,** 39–46
49. Macklon, N. S., and Fauser, B. C. (2001) Follicle-stimulating hormone and advanced follicle development in the human. *Arch. Med. Res.* **32,** 595–600
50. Stouffer, R. L., Xu, F., and Duffy, D. M. (2007) Molecular control of ovulation and luteinization in the primate follicle. *Front. Biosci.* **12,** 297–307
51. Jamnongjit, M., and Hammes, S. R. (2006) Ovarian steroids–the good, the bad, and the signals that raise them. *Cell Cycle* **5,** 1178–1183
52. Jongen, V. H., Hollema, H., Van Der Zee, A. G., and Heineman, M. J. (2006) Aromatase in the context of breast and endometrial cancer. A review. *Minerva Endocrinol.* **31,** 47–60
53. Mishima, T., Takizawa, T., Luo, S. S., Ishibashi, O., Kawahigashi, Y., Mizuguchi, Y., Ishikawa, T., Mori, M., Kanda, T., and Goto, T. (2008) MicroRNA (miRNA) cloning analysis reveals sex differences in miRNA expression profiles between adult mouse testis and ovary. *Reproduction* **136,** 811–822
54. Ahn, H. W., Morin, R. D., Zhao, H., Harris, R. A., Coarfa, C., Chen, Z. J., Milosavljevic, A., Marra, M. A., and Rajkovic, A. (2010) MicroRNA transcriptome in the newborn mouse ovaries determined by massive parallel sequencing. *Mol. Hum. Reprod.* **16,** 463–471
55. Ma, T., Jiang, H., Gao, Y., Zhao, Y., Dai, L., Xiong, Q., Xu, Y., Zhao, Z., and Zhang, J. (2011) Microarray analysis of differentially expressed microRNAs in non-regressed and regressed bovine corpus luteum tissue; microRNA-378 may suppress luteal cell apoptosis by targeting the interferon γ receptor 1 gene. *J. Appl. Genet.* **52,** 481–486
56. Tesfaye, D., Worku, D., Rings, F., Phatsara, C., Tholen, E., Schellander, K., and Hoelker, M. (2009) Identification and expression profiling of microRNAs during bovine oocyte maturation using heterologous approach. *Mol. Reprod. Dev.* **76,** 665–677
57. da Silveira, J. C., Veeramachaneni, D. N., Winger, Q. A., Carnevale, E. M., and Bouma, G. J. (2012) Cell-secreted vesicles in equine ovarian follicular fluid contain miRNAs and proteins: a possible new form of cell communication within the ovarian follicle. *Biol. Reprod.* **86,** 71
58. Yang, X., Zhou, Y., Peng, S., Wu, L., Lin, H. Y., Wang, S., and Wang, H. (2012) Differentially expressed plasma microRNAs in premature ovarian failure patients and the potential regulatory function of mir-23a in granulosa cell apoptosis. *Reproduction* **144,** 235–244
59. Petrocca, F., Visone, R., Onelli, M. R., Shah, M. H., Nicoloso, M. S., de Martino, I., Iliopoulos, D., Pilozzi, E., Liu, C. G., Negrini, M., Cavazzini, L., Volinia, S., Alder, H., Ruco, L. P., Baldassarre, G., Croce, C. M., and Vecchione, A. (2008) E2F1-regulated microRNAs impair TGFβ-dependent cell-cycle arrest and apoptosis in gastric cancer. *Cancer Cell* **13,** 272–286
60. Johnnidis, J. B., Harris, M. H., Wheeler, R. T., Stehling-Sun, S., Lam, M. H., Kirak, O., Brummelkamp, T. R., Fleming, M. D., and Camargo, F. D. (2008) Regulation of progenitor cell proliferation and granulocyte function by microRNA-223. *Nature* **451,** 1125–1129
61. Huang, Q., Gumireddy, K., Schrier, M., le Sage, C., Nagel, R., Nair, S., Egan, D. A., Li, A., Huang, G., Klein-Szanto, A. J., Gimotty, P. A., Katsaros, D., Coukos, G., Zhang, L., Puré, E., and Agami, R. (2008) The microRNAs miR-373 and miR-520c promote tumour invasion and metastasis. *Nat. Cell Biol.* **10,** 202–210
62. Bronisz, A., Godlewski, J., Wallace, J. A., Merchant, A. S., Nowicki, M. O., Mathsyaraja, H., Srinivasan, R., Trimboli, A. J., Martin, C. K., Li, F., Yu, L., Fernandez, S. A., Pécot, T., Rosol, T. J., Cory, S., Hallett, M., Park, M., Piper, M. G., Marsh, C. B., Yee, L. D., Jimenez, R. E., Nuovo, G., Lawler, S. E., Chiocca, E. A., Leone, G., and Ostrowski, M. C. (2012) Reprogramming of the tumour microenvironment by stromal PTEN-regulated miR-320. *Nat. Cell Biol.* **14,** 159–167
63. Feng, B., and Chakrabarti, S. (2012) miR-320 regulates glucose-induced gene expression in diabetes. *ISRN Endocrinol* **2012,** 549875
64. Hsieh, I. S., Chang, K. C., Tsai, Y. T., Ke, J. Y., Lu, P. J., Lee, K. H., Yeh, S. D., Hong, T. M., and Chen, Y. L. (2013) MicroRNA-320 suppresses the stem cell-like characteristics of prostate cancer cells by downregulating the Wnt/β-catenin signaling pathway. *Carcinogenesis* **34,** 530–538
65. Emmrich, S., and Pützer, B. M. (2010) Checks and balances: E2F-microRNA crosstalk in cancer control. *Cell Cycle* **9,** 2555–2567
66. O'Donnell, K. A., Wentzel, E. A., Zeller, K. I., Dang, C. V., and Mendell, J. T. (2005) c-Myc-regulated microRNAs modulate E2F1 expression. *Nature* **435,** 839–843
67. Yang, G., Zhang, R., Chen, X., Mu, Y., Ai, J., Shi, C., Liu, Y., Shi, C., Sun, L., Rainov, N. G., Li, H., Yang, B., and Zhao, S. (2011) miR-106a inhibits glioma cell growth by targeting E2F1 independent of p53 status. *J. Mol. Med.* **89,** 1037–1050
68. Lee, K. H., Chen, Y. L., Yeh, S. D., Hsiao, M., Lin, J. T., Goan, Y. G., and Lu, P. J. (2009) MicroRNA-330 acts as tumor suppressor and induces apoptosis of prostate cancer cells through E2F1-mediated suppression of Akt phosphorylation. *Oncogene* **28,** 3360–3370
69. Tazawa, H., Tsuchiya, N., Izumiya, M., and Nakagama, H. (2007) Tumor-suppressive miR-34a induces senescence-like growth arrest through modulation of the E2F pathway in human colon cancer cells. *Proc. Natl. Acad. Sci. U.S.A.* **104,** 15472–15477
70. Pulikkan, J. A., Dengler, V., Peramangalam, P. S., Peer Zada, A. A., Müller-Tidow, C., Bohlander, S. K., Tenen, D. G., and Behre, G. (2010) Cell-cycle regulator E2F1 and microRNA-223 comprise an autoregulatory negative feedback loop in acute myeloid leukemia. *Blood* **115,** 1768–1778
71. Ofir, M., Hacohen, D., and Ginsberg, D. (2011) MiR-15 and miR-16 are direct transcriptional targets of E2F1 that limit E2F-induced proliferation by targeting cyclin E. *Mol. Cancer Res.* **9,** 440–447
72. Dar, A. A., Majid, S., de Semir, D., Nosrati, M., Bezrookove, V., and Kashani-Sabet, M. (2011) miRNA-205 suppresses melanoma cell proliferation and induces senescence via regulation of E2F1 protein. *J. Biol. Chem.* **286,** 16606–16614
73. Noël, J. C., Borghese, B., Vaiman, D., Fayt, I., Anaf, V., and Chapron, C. (2010) Steroidogenic factor-1 expression in ovarian endometriosis. *Appl. Immunohistochem. Mol. Morphol.* **18,** 258–261
74. Shen, L., Yang, S., Huang, W., Xu, W., Wang, Q., Song, Y., and Liu, Y. (2013) MicroRNA23a and MicroRNA23b deregulation derepresses SF-1 and upregulates estrogen signaling in ovarian endometriosis. *J. Clin. Endocrinol. Metab.* **98,** 1575–1582
75. Sylvestre, Y., De Guire, V., Querido, E., Mukhopadhyay, U. K., Bourdeau, V., Major, F., Ferbeyre, G., and Chartrand, P. (2007) An E2F/miR-20a autoregulatory feedback loop. *J. Biol. Chem.* **282,** 2135–2143
76. Lizé, M., Klimke, A., and Dobbelstein, M. (2011) MicroRNA-449 in cell fate determination. *Cell Cycle* **10,** 2874–2882
77. Kumar, T. R., Wang, Y., Lu, N., and Matzuk, M. M. (1997) Follicle stimulating hormone is required for ovarian follicle maturation but not male fertility. *Nat. Genet.* **15,** 201–204
78. Amsterdam, A., and Selvaraj, N. (1997) Control of differentiation, transformation, and apoptosis in granulosa cells by oncogenes, oncoviruses,

and tumor suppressor genes. *Endocr. Rev.* **18,** 435–461
79. Thompson, E. A., Jr., and Siiteri, P. K. (1974) The involvement of human placental microsomal cytochrome P-450 in aromatization. *J. Biol. Chem.* **249,** 5373–5378
80. Shimasaki, S., Zachow, R. J., Li, D., Kim, H., Iemura, S., Ueno, N., Sampath, K., Chang, R. J., and Erickson, G. F. (1999) A functional bone morphogenetic protein system in the ovary. *Proc. Natl. Acad. Sci. U.S.A.* **96,** 7282–7287
81. Yao, N., Yang, B. Q., Liu, Y., Tan, X. Y., Lu, C. L., Yuan, X. H., and Ma, X. (2010) Follicle-stimulating hormone regulation of microRNA expression on progesterone production in cultured rat granulosa cells. *Endocrine* **38,** 158–166